Materials Advances

REVIEW

View Article Online
View Journal | View Issue

Cite this: *Mater. Adv.*, 2026, 7, 109

Recent advances and challenges in graphene-based nanomaterials for photocatalytic CO_2 reduction

Abhishek R. Patel, [a] Anas D. Fazal, [a] Trupti D. Solanky, [a] Subhendu Dhibar, [b] Sumit Kumar *[c] and Sumit Kumar Panja *[a]

Received 14th July 2025,
Accepted 12th November 2025

DOI: 10.1039/d5ma00750j

rsc.li/materials-advances

Photocatalytic CO_2 reduction is a viable solar-driven approach to sustainably synthesize fuels and chemicals, which provides great potential in response to the urgent threat posed by increasing atmospheric CO_2 levels. Recently, graphene-based nanomaterials have emerged as promising material due to their large surface area, superior electrical conductivity and tunable electrical properties. This study highlights the new developments in graphene-based photocatalysts for CO_2 reduction, including fundamental reaction mechanisms, thermodynamics, kinetics as well as light-induced charge separation. The presentation assesses different forms of graphenes (graphene oxide (GO), reduced graphene oxide (rGO), doped graphene and 3D graphene) with respect to their synthesis, functionality and role of functionalization, including for co-catalysts. The hybrid materials of graphene with metal oxides, semiconductors, metals, and carbon nitrides, significantly enhances charge transport and catalytic performance. The review critically evaluates the previous findings on the influence of different synthesis methods on morphology and performance and includes mechanistic information from spectroscopic and density functional theory (DFT)-based studies. In addition to advances such as single-atom catalysis, hybrid systems and machine learning-based design, the issues of catalyst stability, scalability and environmental issues are discussed. The review highlights the key pathways for developing graphene-based materials for achieving effective, scalable, and sustainable CO_2 photoreduction.

[a] *Material Chemistry Laboratory, Tarsadia Institute of Chemical Science, Uka Tarsadia University, Maliba Campus, Gopal Vidyanagar, Bardoli-Mahuva Road, Surat-394350, Gujarat, India. E-mail: sumitkpanja@gmail.com*
[b] *Department of Physics, Indian Institute of Technology, Patna-801106, Bihar, India*
[c] *Department of Chemistry, Magadh University, Bodh Gaya-824234, Bihar, India. E-mail: sumitkrmgr@gmail.com*

1. Introduction

Increasing levels of CO_2 in the atmosphere is an important factor associated with global climate change, presenting a massive challenge to human health and environmental systems.[1] CO_2 emissions have dramatically increased in the

Abhishek R. Patel

Mr Abhishek Rajeshbhai Patel received his BSc degree from Veer Narmad South Gujarat University in 2021 and MSc (Specialization in Organic Chemistry) from Uka Tarsadia University in 2023. He is currently pursuing his doctoral research under the supervision of Dr Sumit K. Panja at the Tarsadia Institute of Chemical Science, Uka Tarsadia University. His research interests focus on the synthesis and photophysical study of chiral porous materials (CPMs) and covalent organic frameworks (COFs) and their application as photocatalysts for H_2O_2, H_2 evolution and storage.

Anas D. Fazal

Mr Anas D Fazal received his BSc degree (2018–2021) and MSc (2021–2023; Specialization in Organic Chemistry) from Uka Tarsadia University, Bardoli-Surat-394350, Gujarat, India. He is currently pursuing his doctoral research under the supervision of Dr Sumit K. Panja at the Tarsadia Institute of Chemical Science, Uka Tarsadia University. His research interests focus on the solvation dynamics of push–pull organic molecules, dye-sensitized solar cells (DSSCs), and ionic liquids.

past century due to fossil fuel combustion, industrial processes and changes in land-use that have resulted in significant increases in global temperatures, extreme weather events as well as ocean acidification.[2] Therefore, it is critical to reduce CO_2 levels in order to achieve better climatic stability and ultimately sustainability.[3] Photocatalysis employs semiconductors to absorb light, resulting in the formation of electron–hole pairs that drive cellular redox processes to convert CO_2 into hydrocarbon species such as methane, methanol and formic acid.[4,5] Although this research area has attracted considerable attention, its progress is frequently limited by issues such as low conversion efficiency, poor selectivity, and the rapid recombination of photo-generated charge carriers.

Recently, graphene-based nanomaterials have attracted great attention as new components for photocatalytic systems.[6] Graphene-based materials, in particular graphene and its derivatives, *e.g.*, GO, rGO and functionalized hybrids, have shown great potential to enhance the photocatalytic performance based on a multitude of properties when compared to more traditional photocatalysts including the large surface area-to-mass ratio, high electron mobility, chemical stability/tolerance towards oxidation and the ease of modification of surface chemistry.[7,8]

Trupti D. Solanky

Ms Trupti Dilipsinh Solanky obtained her BSc degree from Veer Narmad South Gujarat University in 2019, followed by an MSc in Organic Chemistry from Uka Tarsadia University in 2021. She is presently pursuing her doctoral studies under the guidance of Dr Sumit K. Panja at the Tarsadia Institute of Chemical Science, Uka Tarsadia University. Her doctoral research is centred on the design, synthesis, and photophysical investigations of solvatochromic fluorescent materials, covalent organic frameworks (COFs), and metal–organic frameworks (MOFs), with a particular emphasis on exploring their potential in photonic devices, advanced optical materials, and photocatalytic applications for H_2O_2 evolution and storage.

Subhendu Dhibar

Dr Subhendu Dhibar was born in 1991 in Purandarpur, Birbhum, West Bengal, India. He obtained his PhD in Chemistry from Visva-Bharati University, India, in 2020, with a specialization in supramolecular materials. Following his doctoral studies, he was awarded the prestigious Dr D. S. Kothari Postdoctoral Fellowship and subsequently joined the research group of Prof. Bidyut Saha in the Department of Chemistry at the University of Burdwan, India. He is currently a DST-CSRI Postdoctoral Fellow in Prof. Soumya Jyoti Ray's research group at the Indian Institute of Technology (IIT) Patna, Bihar, India. He is actively involved in interdisciplinary research related to biomedicine, electronics, and environmental science, with a particular focus on the design of self-healing metallogels and the development of Schottky barrier diode-based adaptive electronic devices.

Sumit Kumar

Dr Sumit Kumar is an Assistant Professor in the Department of Chemistry, Magadh University, Bodh Gaya, Bihar, India. He obtained his PhD in Chemistry from the Indian Institute of Science Education and Research (IISER), Pune, in 2014, followed by three years of postdoctoral research at the Max Planck Institute for Multidisciplinary Sciences, Göttingen, Germany. His research interests include materials science, high-resolution spectroscopy, and theoretical chemistry. He is a lifetime member of several professional organizations, including the Indian Science Congress, the Association of Chemistry Teachers (ACT), the Society of Materials Chemistry (SMC), and the Researchers Society of Chemical Sciences.

Sumit Kumar Panja

Dr Sumit Kumar Panja is presently working as an Assistant Professor at the Tarsadia Institute of Chemical Science, Uka Tarsadia University, Surat-394350, Gujarat, India. After finishing his PhD from Banaras Hindu University, India (2011–2016), he moved to the Department of Inorganic and Physical Chemistry, Indian Institute of Science (IISc), Bangalore, India, for postdoctoral work (2016–2018). His research interests include photophysical studies of organic materials, solvation dynamics, organic semiconductors, solar cells, OLED materials, covalent organic frameworks (COFs), metal–organic frameworks (MOFs), and H_2O_2 and H_2 evolution.

Graphene-based materials may enhance photogenerated charge separation, enhance light absorption spectra and improve CO_2 adsorption to overcome limitations in more traditional photocatalyst systems.[9–11]

There is now considerable interest from the scientific community in investigating graphene-based nanomaterials for photocatalytic CO_2 reduction, and we have already seen significant increases in publications and research activities in the past ten years. Interest in the area was less significant after 2015, though prior to that research on graphene-based photocatalysts was also pretty limited, more so in and around 2010.[12,13] This largely came down to the outcome that the coupling of photocatalytic systems with graphene was a relatively new process and mechanism. As the researchers recognized the potential of the electrical properties, functionalities, large surface area and unique role as an electron mediator, the pressure to research increased. After the cumulative number of research papers on graphene in photocatalytic systems peaked around 2015, pressure again began to build due to global climate crisis challenges, with an especially high need for improvements in sustainable energy technology (to at least align in the same direction as work carried out in fulfilling the promise of advancements in hydrocarbon energy technologies). Newer syntheses, improved quality of graphene and hybrid photocatalysts between semiconductor materials (*i.e.*, TiO_2 and g-C_3N_4) and MOFs created new constructive waves in the research environment.[14–16]

In the past few years, the number of publications has generally gone up with high-quality journals in disciplines of physics, chemistry and environmental engineering, and material chemistry *etc*. due to the multidisciplinary nature (Fig. 1). Overall, converging assumptions point towards a maturing technological state and teaching a collaborative approach to research devoted to using graphene and graphene nanostructures in purposeful experiences containing photocatalytic reactions aimed at reduction for possible commercialization toward carbon neutral and carbon negative technologies.

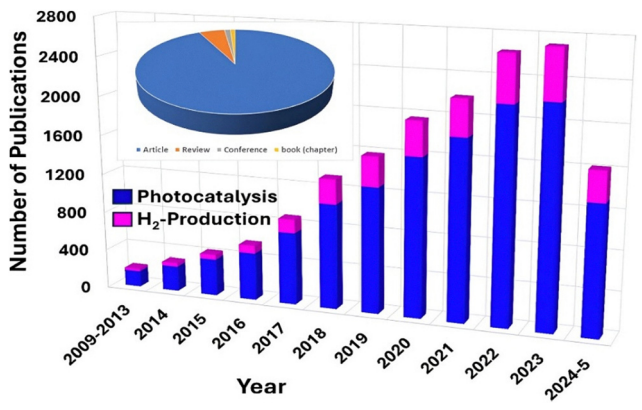

Fig. 1 Publications per year about graphene-based nanomaterials for photocatalytic reduction of CO_2. Reprinted from ref. 17, copyright@2024, RSC.

This study reviews the recent developments in graphene-based nanomaterials use in CO_2 reduction by photocatalytic processes. It reviews the different types of graphene composites and how they can enhance photocatalytic activity (and the scientific principles), addresses current challenges, compares performance between systems and discusses subsequent research avenues to advance this exciting subject into real-life and industrial applications.

2. Fundamentals of photocatalytic CO_2 reduction

2.1 Basic principles and reaction mechanisms

To initiate redox reactions in the surface-driven, light-induced process of photocatalytic CO_2 reduction, semiconductors are used as photocatalysts that absorb photons.[18,19] The photons excite electrons (e^-) in the valence band (VB) to the conduction band (CB) as long as they have an energy equal to or greater than the bandgap energy (E_g) of the photocatalyst. When an electron is promoted to the CB, a hole (h^+) is created in the VB and the VB is now positively charged.

$$\text{Semiconductor} + h\nu \rightarrow e^-(\text{CB}) + h^+(\text{VB})$$

The holes tend to participate in water oxidation to provide protons and maintain charge neutrality, while the photogenerated electrons can thermally decompose the significantly adsorbed CO_2 molecules.[20,21] Depending upon the particular nature of the catalyst and reaction conditions, the reduction of CO_2 may follow a number of paths with potentially complex multi-electron transfer steps.

$$CO_2 + 2H^+ + 2e^- \rightarrow CO + H_2O \quad (E^0 = -0.53\ \text{V } \textit{vs.}\ \text{NHE})$$

$$CO_2 + 2H^+ + 2e^- \rightarrow HCOOH \quad (E^0 = -0.61\ \text{V})$$

$$CO_2 + 8H^+ + 8e^- \rightarrow CH_4 + 2H_2O \quad (E^0 = -0.24\ \text{V}).$$

These reactions are thermodynamically uphill and require catalysts that can facilitate multi-elecon processes with minimal energy input and shown in (Fig. 2).[20]

2.2 Thermodynamics and kinetics of CO_2 photoreduction

CO_2 is a linear and stable compound with a strong C═O bond (bond energy of 750 kJ mol^{-1}), and it is difficult to activate.[23,24] Thermodynamic reductions of CO_2 to products such as CO, CH_4 or CH_3OH must overcome significant energy barriers and be utilized in conjunction with the redox potentials of the photocatalyst (Fig. 3). In terms of kinetic functionality, the pathway to CO_2 reductions competes with the hydrogen evolution reaction (HER), which is often thermodynamically favourable.[25]

Therefore, kinetic control through catalyst surface modification, active site engineering and selective adsorption of CO_2 *vs.* H^+ is important to increase selectivity.[27] Additionally, product formation is very sensitive to the number of electrons transferred: CO and HCOOH are $2e^-$ products, while CH_4 and

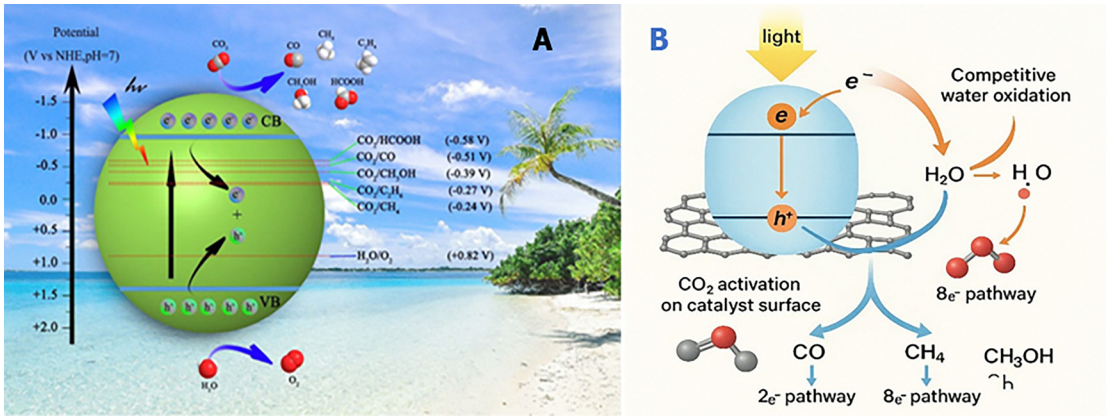

Fig. 2 (A) Band edge alignment and redox potentials for the photocatalytic CO_2 reduction with H_2O. (B) General mechanism of the graphene-based photocatalytic CO_2 reduction pathways. Reprinted from ref. 22, copyright@2020, RSC.

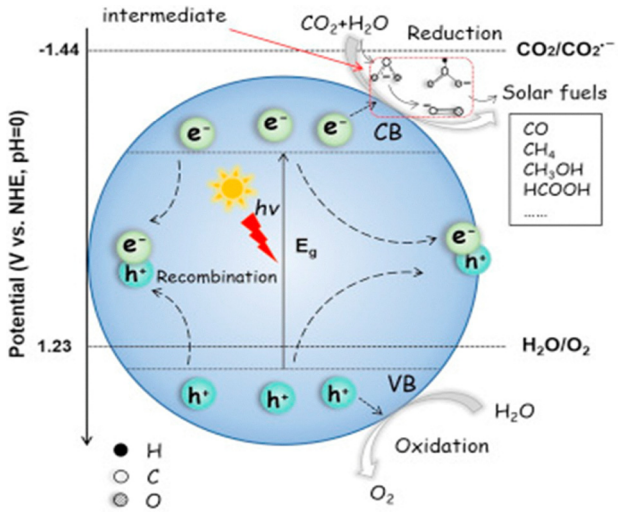

Fig. 3 Schematic of the thermodynamics and kinetics of CO_2 photoreduction. Reprinted from ref. 26, copyright@2020, Elsevier.

CH_3OH are $8e^-$ and $6e^-$ products, respectively, making this kinetically more complicated.

2.3 Desired products and selectivity control reactions

Selectivity remains a central challenge in photocatalytic CO_2 reduction due to the coexistence of multiple reaction intermediates (COOH, CHO, and CH_2OH) and competing reduction pathways that lead to diverse products.[28,29] Depending on the stabilization and transformation of these intermediates, the system can yield CO, HCOOH, CH_4, or CH_3OH, which serve as valuable chemical feedstocks, hydrogen carriers or high-energy density fuels. However, the intrinsic competition with the hydrogen evolution reaction (HER) and the difficulty in controlling electron–proton transfer steps often result in poor product distribution and low carbon efficiency. Consequently, improving product selectivity is not merely a matter of enhancing catalytic activity but also a matter of directing the reaction mechanism toward well-defined and desirable pathways, which is essential for practical applications in solar-to-fuel conversion.

A variety of strategies have been developed to enhance selectivity in CO_2 photoreduction. Catalyst composition and morphology play a pivotal role, where controlled doping with transition metals or nonmetals modulates electronic structures and adsorption energies, thereby stabilizing key intermediates and suppressing side reactions.[30] Similarly, rational engineering of the electronic band structure governs the separation and distribution of photogenerated charge carriers, influencing surface coverage and the reduction potential available for CO_2 activation.[31] Beyond intrinsic material properties, the introduction of surface functional groups provides specific anchoring sites that stabilize critical intermediates, improving the probability of their conversion into targeted products. In addition, external factors such as electrolyte pH, CO_2 partial pressure and the incorporation of co-catalysts can further tune the reaction kinetics, facilitating selective product formation under optimized operating conditions.[32]

Graphene-based materials have emerged as highly effective platforms for improving selectivity in CO_2 reduction owing to their unique physicochemical features. The conjugated π-network and superior electron mobility of graphene enable rapid charge transfer and efficient stabilization of electron-rich intermediates, thereby minimizing unwanted back-reactions. Furthermore, the tunability of graphene through heteroatom doping, covalent functionalization, and formation of heterostructures provides versatile pathways to modulate the CO_2 adsorption strength and intermediate stabilization. These attributes, combined with graphene's ability to integrate synergistically with semiconductors and metal nanoparticles, make graphene-based photocatalysts promising candidates for achieving high selectivity toward desired products, thus offering a rational route toward efficient and sustainable CO_2-to-fuel conversion.

2.4 Role of light harvesting and charge separation

To use the photocatalytic process effectively, good light harvesting is important. Ideally, photocatalysts should absorb a wide spectral extent, especially in the visible region (~400–700 nm) where most solar energy is located.[28,29] Many traditional

photocatalysts (such as TiO_2) have large bandgaps (>3.0 eV) that prevent further efficient use of sunlight.[30]

Since photogenerated electron–hole pairs rapidly recombine and this can drastically reduce the quantum efficiency, charge separation efficiency is thus also very important and shown in Fig. 4.[32] The following are some strategies for increasing light absorption and reducing recombination. The overall performance of photocatalytic systems is characterized by the synergy that can be established through increased light absorption, rapid charge carrier mobility and CO_2 adsorption on catalyst surfaces.[33,34]

2.4.1 Factors and areas of consideration. Bandgap engineering has been widely recognized as a fundamental strategy for improving photocatalytic CO_2 reduction efficiency. By tailoring the band structure, photocatalysts can extend their light absorption into the visible range while maintaining the redox potentials required for CO_2 activation and subsequent multi-electron transfer processes. Techniques such as heteroatom doping introduce impurity energy levels that narrow the bandgap and tune the electronic structure, while the construction of heterojunctions between semiconductors creates internal electric fields that facilitate charge separation. These modifications not only improve solar spectrum utilization but also influence the adsorption and stabilization of key intermediates, thereby enhancing both activity and selectivity. In particular, graphene-based heterojunctions with semiconductors provide unique advantages by integrating extended light absorption with efficient charge transport pathways.

Z-scheme photocatalytic systems represent another promising approach, drawing inspiration from the architecture of natural photosynthesis. In these systems, two semiconductors are coupled in a manner that maintains the strong reduction potential of one and the strong oxidation potential of the other, while photogenerated electrons and holes in the less energetic bands recombine internally. This spatial and energetic separation allows for simultaneous CO_2 reduction and water oxidation with high efficiency. Incorporating graphene into Z-scheme systems further enhances their performance, as graphene can act as a solid-state conductive bridge, promoting ultrafast charge transfer while suppressing recombination. Recent studies have demonstrated that such graphene-based Z-scheme systems exhibit superior stability and selectivity compared to conventional type-II heterojunctions, making them highly attractive for solar fuel production.

Surface plasmon resonance (SPR) effects associated with noble-metal decoration provide an additional avenue for enhancing photocatalytic CO_2 reduction. Metals such as Au, Ag, and Cu can generate localized electromagnetic fields under light irradiation, leading to strong absorption in the visible region and the excitation of high-energy "hot" electrons. These hot carriers can be injected into adjacent semiconductors or graphene-based supports, where they participate directly in CO_2 reduction reactions. Moreover, the synergistic combination of plasmonic metals with graphene facilitates rapid hot-electron transfer due to the high conductivity and extended π-conjugation of graphene, thus suppressing charge recombination and improving reaction selectivity. Graphene serves as an electron sink and conductive channel for showing the spatial charge separation dynamics across hybrid interfaces. Together, bandgap engineering, Z-scheme architectures, plasmonic enhancement, and graphene-mediated charge transport constitute complementary and mutually reinforcing strategies that can be rationally combined to overcome the efficiency and selectivity bottlenecks in photocatalytic CO_2 conversion.

Although notable progress has been made with traditional photocatalysts for CO_2 reduction, their overall efficiency is still restricted by inherent challenges such as fast charge carrier recombination, narrow light absorption, and a limited number of surface-active sites for CO_2 activation. To overcome these drawbacks, researchers have increasingly focused on graphene and graphene-based nanomaterials, which offer outstanding electrical conductivity, large specific surface area, and chemically tunable interfaces. These features facilitate efficient charge separation and transfer, enhanced light harvesting when coupled with semiconductors, and improved catalytic reactivity. The subsequent section will provide an in-depth discussion of the structure, properties, and photocatalytic roles of graphene and its derivatives in advancing CO_2 conversion technologies.

3. Graphene and graphene-based nanomaterials

3.1 Structure and properties of graphene

Graphene is a 2D carbon allotrope made up of a single atomic layer of sp^2-hybridized carbon atoms arranged in a honeycomb

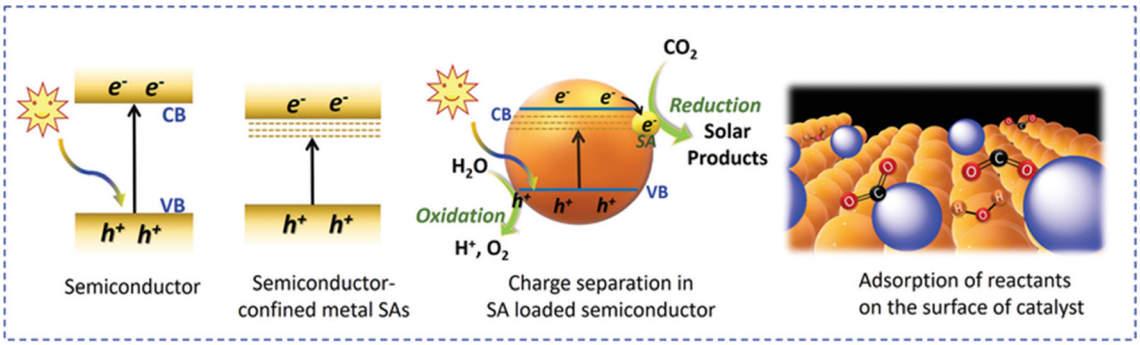

Fig. 4 Schematic of light harvesting and charge separation. Reprinted from ref. 31, copyright@2020, Wiley Online Library.

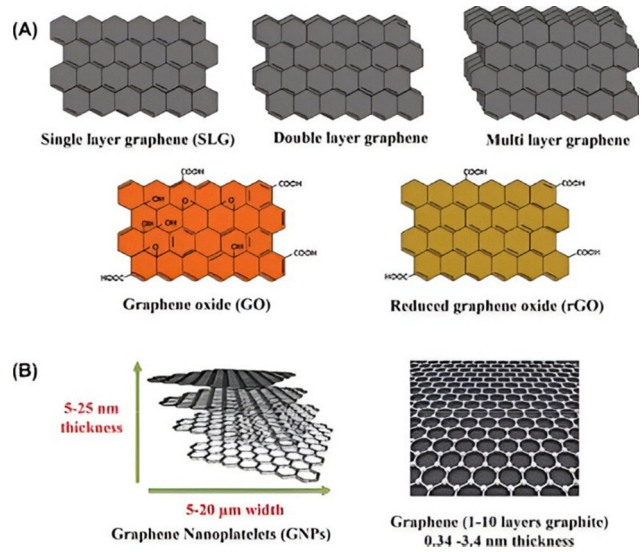

Fig. 5 (A) Different structural forms of graphene and its derivatives: single-layer graphene (SLG), double-layer graphene, multi-layer graphene, GO with oxygen-containing functional groups, and RGO with partially restored graphitic structure. (B) Morphological representations of the graphene-based materials: graphene nanoplatelets (GNPs) with 5–25 nm thickness and 5–20 μm lateral size; few-layer graphene (1–10 layers) with a thickness of 0.34–3.4 nm. Reprinted from ref. 39, copyright@2019, Dove Medical Press.

lattice, as shown in Fig. 5.[35] This unique atomic arrangement endows graphene with many exceptional physicochemical properties that make it a much-studied material with significant potential for a wide range of applications including photocatalysis.[36] Logically, every carbon atom is connected to three neighbours in graphene, forming a stable and delocalized π-electron system across the entire sheet.[37] The delocalization of electrons leads to the desired properties of graphene electroconductivity, thermal stability, and typical mechanical stability. For example, the intrinsic carrier mobility of graphene at room temperature is above 200 000 $cm^2\ V^{-1}\ s^{-1}$, with a thermal conductivity beyond 5000 $W\ m^{-1}\ K^{-1}$. Graphene also has excellent flexibility and only absorbs ~2.3% of visible light, giving it apparent transparency, such as for optical electronic applications. It has the theoretically highest surface area: 2630 $m^2\ g^{-1}$ (simply meaning a large surface area for chemical reactions or adsorption).[38]

The unique characteristics make graphene a perfect medium for electron transport and interfacial charge transfer processes specifically, which is vital for photocatalytic processes.[40] However, pristine graphene is chemically inert; therefore, it lacks a bandgap which prevents it from being useful by itself in this area of electronics.[41] Therefore, researchers have looked into graphene-based derivatives and composites to both overcome the limitations of pristine graphene and take advantage of its conductive and mechanical properties.

3.2 Derivatives of GO, rGO, doped graphene, and 3D graphene

To prepare graphene for real photocatalytic and catalytic applications, numerous derivatives have been created.[42] The goals of the derivatives generally relate to introducing chemical functionalities, creating a bandgap, increasing dispersibility in solvents, and establishing synergistic effects with other catalytic materials.[43]

GO is a heavily oxidized version of graphene, with many oxygen-containing functional groups (*e.g.*, hydroxyl, epoxy, and carboxyl) attached to its sheet structure (Fig. 6). These oxygen-containing groups disrupt the conjugated π-electron system (cause pi conjugation to cease), thereby diminishing the electrical conductivity of GO, but markedly increasing its hydrophilicity and chemical reactivity.[44] GO is easily dispersible in water and other polar protic solvents, thereby enabling its use as an important scaffolding material to support subsequent growth and immobilization of photocatalysts.[45] Importantly, GO, when incorporated to make a composite material with photocatalysts, shows improved interfacial interactions, charge transfer and increased photocatalytic activity due to its higher density of functional groups and defect sites.[46]

RGO can be chemically, thermally or electrochemically reduced GO leaving behind a partially restored π-conjugated network, some reduction in the oxygen content and the possibility of partially restoring GO electrical conductivity, making rGO a better candidate for electron mediator than GO itself.[47] The reduction also creates defects and residual functional groups that can impact interfacial properties and device performance. However, rGO provides a balance between good conductivity and sufficient surface functional groups, when surface functionality is important in encapsulating many photocatalytic systems (Fig. 7).[48]

Doped graphene is graphene with heteroatoms (like nitrogen (N), boron (B), sulphur (S) or phosphorus (P)) incorporated into the lattice as a substituent of carbon atoms or attached to the surface (Fig. 8). Doping creates changes in the electronic structure of graphene, creating localized states within the bandgap and changing work function of the graphene.[50,51] For example, N-doped graphene has been shown to have better electron donor ability, so some of doped graphene's interactions increase the catalytic reaction activity and lead to an increased interaction with nanoparticles of metals or semiconductors.[52] Each of these changes improves photocatalytic ability, through better charge separation and transfer.

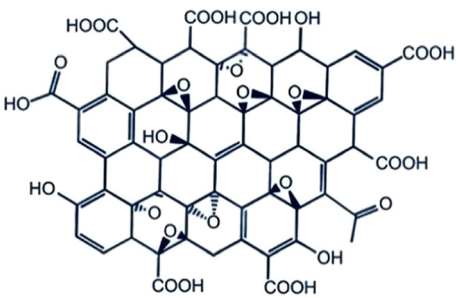

Fig. 6 Structural model of GO showing oxygen-containing functional groups such as hydroxyl (–OH), epoxy (–O–), carbonyl (C═O), and carboxyl (–COOH) distributed on the basal plane and edges of the graphene sheet. Reprinted from ref. 39, copyright@2019, Dove Medical Press.

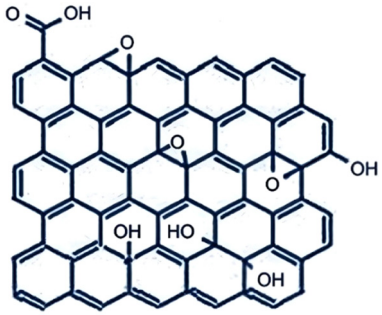

Fig. 7 Structural model of rGO, showing a partially restored sp^2 carbon network with the residual oxygen-containing functional groups such as hydroxyl (–OH), epoxy (–O–), and carboxyl (–COOH) groups remaining on the basal plane and edges. Reprinted from ref. 39, copyright@2019, Dove Medical Press.

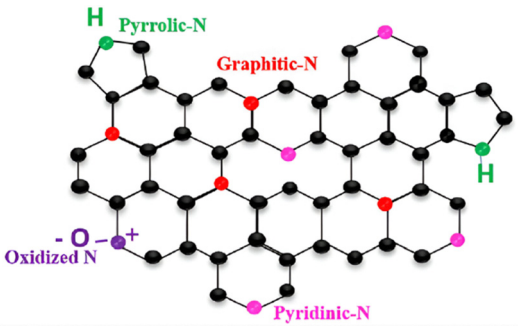

Fig. 8 Schematic of the nitrogen-doped graphene showing different nitrogen configurations, including pyridinic-N, pyrrolic-N, graphitic-N, and oxidized-N within the graphene lattice. These doped sites significantly influence the electronic structure, surface reactivity, and catalytic activity of the graphene-based materials. Reprinted from ref. 49, copyright@2021, Springer.

Three-dimensional (3D) graphene architectures[54] (*e.g.*, graphene aerogels, foams, and hydrogels) provide a macroporous and mesoporous scaffold, high surface area, significantly enhanced mechanical stability and favourable mass transport properties (Fig. 9).[55–57] These traits can be leveraged to support photocatalytic nanoparticles and encourage light absorption and reactant diffusion.[46] Furthermore, these 3D graphene support materials can provide continuous conductive pathways for charge migration, which will help reduce the electron–hole recombination.[56]

In general, these graphene-based nanomaterials can be intelligently chosen or designed based on the requirements of the photocatalytic system, for example, light absorption capabilities, charge transportation features, reactant adsorption and/or interfacial interactions.

3.3 Methods of synthesis and functionalization of graphene and its derivatives

Graphene and its derivatives have unique physicochemical properties that can be synthesized and functionalized to enhance those properties and tailor them for specific applications.[57] This is particularly appropriate for photocatalysis for CO_2 reduction. Graphene synthesis is separated into two major categories: – top down and bottom up (Fig. 10).[58]

The top-down method involves the exfoliation of bulk graphite into single individual graphene sheets.[60] Mechanical exfoliation can produce high-quality graphene, but is not scalable. Chemical exfoliation methods, like the Hummers' method and its variations, are often employed for GO synthesis. Chemical exfoliation uses powerful oxidizing agents (*e.g.* $KMnO_4$ and H_2SO_4) in the oxidation of graphite by adding oxygenated groups which separate the interlayers and promote exfoliation. The GO produced can then be reduced to rGO *via*

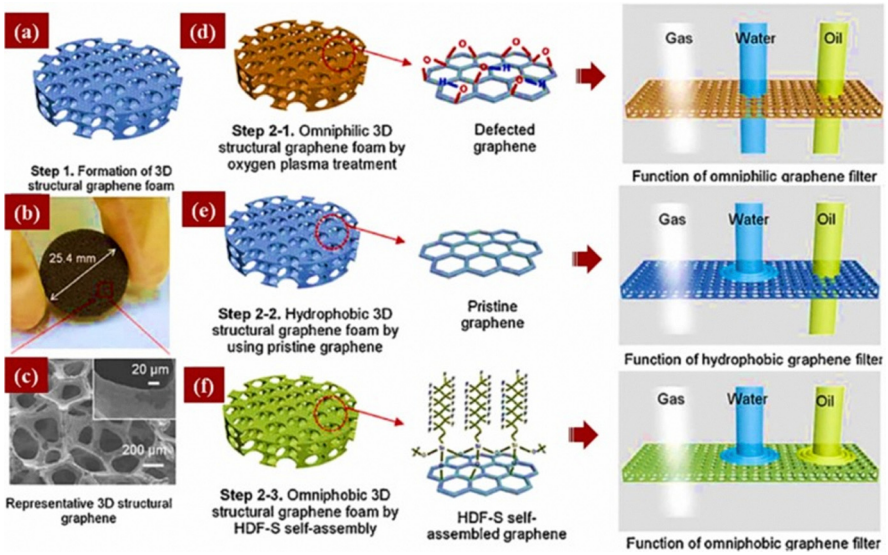

Fig. 9 Graphene foam contains various functional groups for use in the selective separation of gas, water, and oil. (a) Structure of graphene-foam. (b) Three-dimensional graphene foam picture. (c) SEM-micrograph porous structures. (d) Gas, water, and oil travel through deformed graphene. (e) Pure graphene foam accepts gas and oil yet blocks water. (f) HDF-S-covalently bonded graphene can filter gases. Reprinted from ref. 53, copyright@2018, Wiley Online Library.

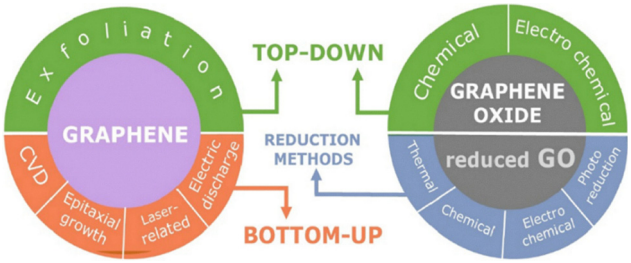

Fig. 10 Methods of synthesis and functionalization of graphene and its derivatives. Reprinted from ref. 59, copyright@2022, Springer.

chemical (*e.g.* hydrazine and ascorbic acid), thermal, or electrochemical routes.[61]

Bottom-up methods use graphene from molecular precursors, generally through chemical vapor deposition. Chemical vapor deposition puts graphene films into high-purity, large-area films on metal substrates (Cu or Ni).[62] CVD has great potential in different electronic and optoelectronic applications, but it is not considered practical for the production of graphene-based photocatalytic composites due to cost and scalability.[59]

The functionalization of graphene is necessary to bring usable chemical groups, improve compatibility with other materials, and ultimately improve electronic properties.[63] Covalent functionalization occurs the when chemical bond to the carbon lattice (often through reactions with the oxygenated groups in GO, for example) provides stable bonds and improved dispersibility for composites; however, this process may limit the use of the conjugated structure of graphene and limit conductivity. Non-covalent functionalization generally introduces molecules or nanoparticles from the enveloping compound to the sp^2 framework of graphene through π–π interactions, hydrogen bonding and/or electrostatic interactions.[64,65]

In photocatalytic applications, functionalization strategies usually consist of decorating graphene with metal or metal oxide nanoparticles (TiO_2, ZnO or CdS); anchoring co-catalysts; or doping with heteroatoms to improve the potential of light absorption, reactive sites and charge separation.[66] Generally, methods of synthesis/functionalization are the major factors in impacting the overall performance of the synthesized graphene-based composites.

3.3.1 Chemical synthesis methods for graphite oxide. Extensive research has focused on understanding the structure of GO, the primary precursor of graphene materials. GO is typically synthesized by intercalating and oxidizing graphite powder using strong acids (*e.g.*, HCl, H_2SO_4, and HNO_3) and oxidizing agents (*e.g.*, $NaNO_3$, $KMnO_4$, and $KClO_3$). Several chemical synthesis methods are discussed in Table 1. Each method differs in its oxidants, advantages, disadvantages, and resulting carbon-to-oxygen (C/O) ratios.

Brodie's oxidation method was the first to synthesize GO by reacting graphite with $KClO_3$ along with HNO_3 at around 60 °C for three to four days.[67,68] The process involved repeated oxidation steps and drying at 100 °C. Although effective, it has major drawbacks including long reaction times and the emission of toxic gases.

The Staudenmaier method improved Brodie's process by using a mixture of concentrated HNO_3, H_2SO_4, and gradually added $KClO_3$ to achieve higher oxidation in a single vessel.[69] The reaction involved controlled heating, stirring, and subsequent cooling with water, which is followed by filtration and washing. It produces highly oxidized GO but major disadvantages are long reaction times, explosion risks, and toxic chlorine gas release.

Table 1 Summary of synthesis methods and their impact on catalytic performance

SN.	Synthesis method	Typical procedure	Surface area	Defect density	Impact on catalytic activity	Remarks	Ref.
1	Hummers' method (chemical oxidation/reduction)	Oxidation of graphite → Graphene oxide → Reduction to rGO	Moderate–high (depends on reduction)	High (due to oxygen functional groups, vacancies)	Enhances active sites and electron transfer but may introduce recombination centers	Common, scalable; quality depends on reduction degree	82
2	Hydrothermal/solvothermal	Graphene oxide mixed with precursors, treated at high *T* and *P*	High (porous, few-layer structures)	Moderate (controlled defect formation)	Good dispersion of co-catalysts, strong interfacial contact improves activity	Suitable for hybrids (*e.g.*, graphene–metal oxides)	83
3	Chemical vapor deposition (CVD)	Hydrocarbon gases decomposed on metal substrate	Very High (high crystallinity, large domain size)	Low (near defect-free)	Excellent charge transport; but fewer catalytic sites unless doped/functionalized	Expensive, limited scalability	84
4	Exfoliation (liquid phase or electrochemical)	Sonication, shear, or electrochemical delamination of graphite	Moderate–high (depends on exfoliation efficiency)	Variable (controlled *via* process)	Balances conductivity and defect density, useful for heterojunctions	Green methods possible; lower yield than chemical oxidation	85
5	Doping-assisted synthesis (N, S, B, P doping)	Graphene prepared with heteroatoms introduced during synthesis or post-treatment	Moderate	Controlled defect sites (heteroatom-induced)	Creates active sites, improves CO_2 adsorption and electron transfer	Strongly enhances selectivity for CO/CH_4	86

Original Hummers' method introduced a faster and safer alternative for synthesizing GO using $KMnO_4$ and $NaNO_3$ as oxidants in conc. H_2SO_4 with graphite.[70] The reaction proceeds through controlled temperature stages (0–4 °C, 35 °C, and 98 °C). It takes about two hours. After oxidation, H_2O_2 is added to reduce residual manganese compounds, followed by washing and drying to obtain GO. The mechanism involves four stages, which are intercalation, convection-diffusion, oxidation and purification. During intercalation, H_2SO_4 and $NaNO_3$ generate HNO_3 and reactive oxygen species that open graphite layers. $KMnO_4$ reacts with H_2SO_4 to form Mn_2O_7, which intercalates between layers in the step of convection-diffusion. Further Mn_2O_7 decomposes into O_2 and O_3, oxidizing graphite into graphite oxide. The purification is performed using H_2O_2 and HCl, and it removes residual manganese compounds.

Improved Hummers' methods aim to enhance the efficiency, yield, and environmental safety while reducing toxic emissions. These modifications fall into several main categories.

H_2SO_4/$KMnO_4$-based methods eliminate $NaNO_3$, preventing toxic NO_2/N_2O_4 release without reducing the yield.[71] It enables large-scale, eco-friendly GO synthesis, with oxidation levels adjustable by the $KMnO_4$ concentration and drying temperature. H_2O_2 acts as a terminating agent, and its quantity influences the C/O ratio. The reaction involves three stages: acid intercalation, oxidation to pristine graphite oxide, and hydration to form GO. A "mild oxidation" variant (lower $KMnO_4$ ratio) yields more crystalline, water-dispersible GO suitable for high-conductivity graphene.

Introduced by Marcano *et al.*, H_2SO_4–H_3PO_4/$KMnO_4$-based methods replace $NaNO_3$ with a 9 : 1 H_2SO_4 : H_3PO_4 mixture, increasing the oxidation efficiency and yield while eliminating toxic gas formation.[72] It allows better temperature control (35–50 °C) and produces three times more GO than the original method. Further optimization studies refined intercalators and drying steps for faster, cost-effective, and scalable production.

In case of ferrate-assisted oxidation, $KMnO_4$ is partially replaced with K_2FeO_4, which has a higher oxidizing power and operates under milder conditions (<5 °C, 35–95 °C), improving the efficiency while reducing acid use and environmental impact. During $KMnO_4$-free methods, eco-friendly alternatives such as K_2FeO_4, ozone, peracetic acid, and electrochemical oxidation avoid toxic manganese by-products. Though oxidation levels may be lower, these methods offer safer, scalable production routes.

Microwave-assisted oxidation approach rapidly heats reactants *via* dielectric heating, reducing the synthesis time from several days to about 20 minutes at 100 °C. It yields GO with higher C/O ratios (less oxygenated) but is significantly faster and energy-efficient.[73,74]

3.4 Graphene as an electron mediator and co-catalyst

Graphene-based nanomaterials are essential electron mediators and co-catalysts in the context of photocatalytic CO_2 reduction and photocatalysis processes (Fig. 11). Both roles are important for charge separation, interfacial charge transfer, and the recombination suppression of photogenerated electron–hole pairs.[75] As an electron mediator, graphene illustrated an effective electron transport pathway between the photocatalyst and the reaction interface.[76] The high electrical conductivity of graphene and its massive π-conjugated system allows excited electrons to readily transfer from a semiconductor photocatalyst to graphene, a charge sink or electron reservoir, to prevent hole recombination and remain energized carriers.[77] In TiO_2/graphene composites, for example, photogenerated electrons can migrate away from TiO_2 to graphene and, subsequently, to CO_2 molecules disposed on the surface, providing multi-electron reductions. The unique capacity of graphene produced directional charge flow, allowing for the increase in the overall quantum efficiencies of the system.[78,79]

Graphene serves as a support co-catalyst that supplies active sites for adsorption and activation of CO_2 and other materials (Table 1). Functional groups, defects, or impurities (dopants) in the graphene surface can serve as anchoring sites or functional catalytic sites.[76] For example, in nitrogen-doped graphene, the lone pair electrons of nitrogen can react with CO_2 and catalytically activate and reduce it.[78] Metal nanoparticles deposited onto graphene, and the support themselves, can work together to enhance the catalytic activity. The electron-rich graphene substrate can stabilize metal active sites, facilitate charge transfer, and modulate the electronic environment of the catalytic centres.

Graphene composites with semiconductors can form a Schottky junction or heterojunction, which facilitates charge

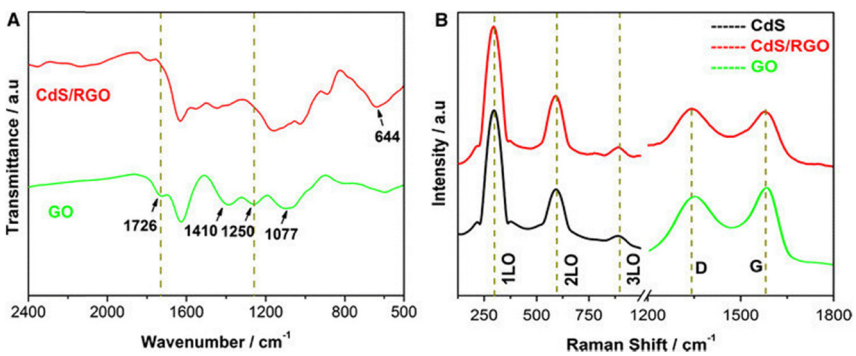

Fig. 11 (A) FT-IR-profiles of GO and CdS-RGO. (B) Raman-spectra of GO, CdS nanoparticles and CdS-RGO. Reprinted from ref. 80, copyright@2020, Springer.

separation and selective pathway for the reaction. CdS/rGO systems provide an example, where rGO facilitates the charge process by improving the mobility of the electrons and also minimizing the photo-corrosive degradation of the CdS material. Similarly, graphene composites with perovskites improve electron transport, enhancing rapid electron transport potential, stability, and superior photocatalytic performance.[75,81]

4. Recent progress in graphene-based photocatalytic systems

Graphene-based materials can benefit photocatalytic systems and help reduce CO_2 levels. When combined with different functional materials such as metal oxides, semiconductors, metals and carbon-based materials, they can result in advanced nanocomposites with better charge separation, light absorption capacity, and surface reaction sites.[87,88] This section will talk about the recent developments in these five fields: graphene/metal oxide nanocomposites, graphene/semiconductor heterojunctions, graphene/metal-based nanohybrids, graphene/carbon nitride and their 2D/2D heterostructures, and graphene-based Z-scheme photocatalytic systems.[89,90]

4.1 Graphene/metal-oxide nanocomposites

Metal oxides are some of the most studied photocatalytic materials due to their advantageous band structures, photostability, and availability including tungsten trioxide (WO_3), zinc oxide (ZnO), and titanium dioxide (TiO_2) (Fig. 12).[91] Unfortunately, the fast recombination of photogenerated charge carriers and the limited visible light absorption often decrease the actual photocatalytic performance of metal oxides. One successful strategy to overcome these limitations has been to combine these systems with graphene.[92]Graphene/metal oxide nanocomposites have emerged as highly effective photocatalytic systems owing to the synergistic effects facilitating charge separation, light absorption, and surface reaction kinetics.[93] In these nanocomposites, graphene behaves as a conductive support and electron mediator, and metal oxides are the primary photocatalysts. Graphene in combination with TiO_2, ZnO, Fe_2O_3, and CuO not only improves photocatalytic performance in CO_2 reduction under UV light but also performs well under visible light.[94,95]

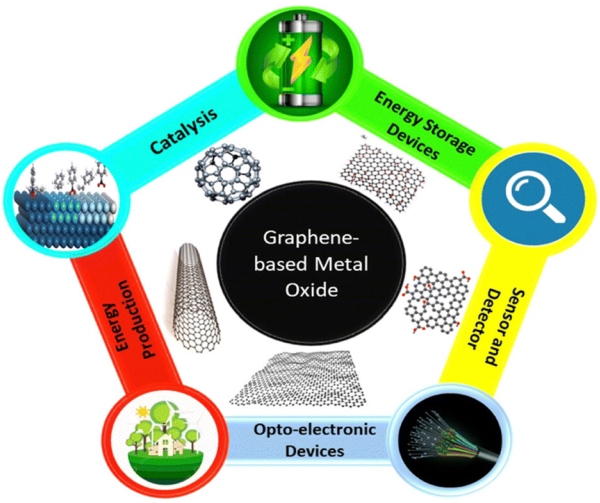

Fig. 12 Nanocomposites of graphene/metal oxide. Reprinted from ref. 96, copyright@2024, RSC.

Graphene/TiO_2 has been studied more than most other systems. Graphene is critical to improving the photocatalytic efficiency of TiO_2, as it increases light absorption in the visible area and reduces electron–hole recombination.[97,98] However, due to the high electron mobility and high surface area of graphene, electrons can be transferred quickly from the TiO_2 conduction band to a graphene sheet to lengthen the life of photogenerated charge carriers. In addition, graphene has multiple active sites for CO_2 adsorption, which is important for increasing the photocatalytic conversion efficiency.[99,100]

Graphene enhances the CO_2 photoreduction activity of many ZnO-based nanocomposites. It is said that the graphene sheets intercalate and transport electrons from heated ZnO, which reduces charge-recombination and improves the production of the key intermediates CO_2^- and $HCOO^-$.[101–104] Because of its π-conjugated electronic framework, graphene can produce enhanced interactions with CO_2 *via* π–π stacking allowing for improved gas collection and activation on its surface.[105] Graphene also enhances the photocatalytic activity of other visible light-responsive metal oxides such as Fe_2O_3 and CuO. Overall, the charge transport and increased absorption of light energy that is seen in graphene/Fe_2O_3 composites comparatively to Fe_2O_3 were probably due to the small bandgap of Fe_2O_3.[106] Graphene performs similarly in the case of CuO as well since the heterojunction also has a considerable charge transport factor while stabilizing reactive species for the CO_2 reduction pathways.[107]

The synthetic methods including hydrothermal synthesis, sol–gel procedures and *in situ* growth are important factors that affect interfacial contact, particle size distribution and electron coupling between graphenes and metal oxides. Efficient charge transport through the nanocomposite is dependent on creating strong interfacial contacts that optimize electron transport pathways and facilitate lower energy barriers for charge migration.[108,109] Graphene/metal oxide nanocomposites are versatile photocatalysts that may be engineered for higher CO_2 conversion performance, by tailoring materials design, *i.e.*, composition, shape, and interfacial properties in unprecedented detail.

Some recent studies have further highlighted the importance of rational design strategies in advancing photocatalytic systems for energy and environmental applications (Table 2). ZnO-based heterostructures continue to attract attention due to their cost-effectiveness and stability, though their intrinsic drawbacks necessitate heterojunction engineering.[110] Both S-scheme and Z-scheme heterostructures have demonstrated exceptional improvements in charge separation and redox capability, with Nb_2O_5/La_2O_3 and ZnO-g-C_3N_4–CuO systems showing outstanding hydrogen evolution rates and strong stability.[111–113] Similarly, the integration of CNTs with Sr-doped ZnO and the ternary ZnO–Cu–CdS composite reveal

Table 2 Comparative performance of the graphene-based photocatalysts for CO_2 reduction

SN	Catalyst system	Synthesis method	CO_2 conversion rate	Product selectivity	Quantum efficiency (QE)	Stability (h)	Ref.
1	rGO–TiO_2 nanocomposite	Hydrothermal assembly (GO + Ti precursor)	~45–80 μmol g^{-1} h^{-1}	CO (70%), CH_4 (20%), H_2 (10%)	0.5–1.2%	15–20 h	116
2	Graphene–ZnO heterojunction	Solvothermal growth of ZnO on GO	~30–60 μmol g^{-1} h^{-1}	CO (65%), CH_4 (25%)	0.3–0.8%	10–15 h	117
3	N-doped Graphene–Cu_2O	In-situ reduction with nitrogen precursor	~120 μmol g^{-1} h^{-1}	CH_4 (55%), CO (40%)	~2.1%	30 h	118
4	Graphene–g-C_3N_4 2D/2D heterostructure	Thermal polymerization of urea + GO	~150 μmol g^{-1} h^{-1}	CO (80%), CH_4 (15%)	~2.5%	40 h	119
5	rGO–Ag–TiO_2 plasmonic system	Photo deposition of Ag NPs on rGO–TiO_2	~200 μmol g^{-1} h^{-1}	CO (90%), trace CH_4	~3.0%	50 h	120
6	Graphene–MoS_2 hybrid	Hydrothermal co-assembly	~100 μmol g^{-1} h^{-1}	CO (75%), CH_4 (20%)	1.8%	25 h	121
7	B-doped Graphene–TiO_2	Sol–gel with boron precursor	~85 μmol g^{-1} h^{-1}	CH_4 (60%), CO (30%)	1.0–1.5%	20 h	122

that synergistic effects between dopants, carbon supports, and mediators such as Cu can significantly enhance light absorption, interfacial charge transfer, and pollutant degradation.[112,114] These advances not only improve photocatalytic efficiency but also broaden application versatility, spanning H_2 production, dye degradation and CO_2 reduction.[115]

4.2 Graphene/semiconductor heterojunctions

Besides the classic metal oxides, graphene has been paired with a number of semiconductors with lower band gaps and tunable properties to generate competitive photocatalytic heterojunctions.[123,124] There have been a large number reporting the hybridization of graphene with the semiconductor's bismuth vanadate ($BiVO_4$), molybdenum disulphide (MoS_2), cadmium sulphide (CdS), and graphitic carbon nitride (g-C_3N_4) along with hybrid hierarchically porous catalytic metal oxides where the changing properties to metal oxides were complimentary as shown in Fig. 13.[125]

Kim *et al.* successfully synthesized ZnO nanostructures with nanoneedle and nanowall morphologies directly on few-layer graphene sheets.[127] In their approach, mechanically exfoliated graphene was transferred onto SiO_2/Si substrates, followed by the growth of ZnO using a metal–organic vapor phase epitaxy (MOVPE) process carried out without any catalyst assistance. The study revealed that both the aspect ratio and spatial arrangement of the ZnO nanostructures—whether aligned vertically or organized in rows—were strongly influenced by the growth temperature, which affected nucleation behavior at the step edges of the graphene surface. Furthermore, the optical characteristics of the ZnO/graphene hybrids were examined through photoluminescence (PL) spectroscopy conducted in the 17–200 K temperature range, providing insights into their structural and electronic quality.

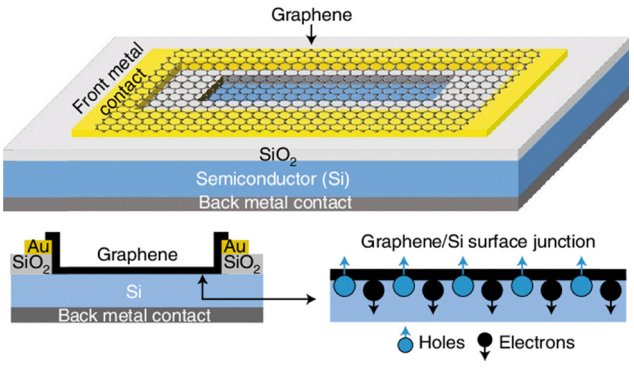

Fig. 13 Schematic of a graphene-on-semiconductor Si heterojunction photovoltaic cell. Reprinted from ref. 126, copyright@2019, Nature.

Zinc sulfide (ZnS), one of the earliest studied semiconductors, shares structural and electronic similarities with ZnO but offers distinct advantages such as wider band gaps (3.72 eV for cubic and 3.77 eV for hexagonal forms), making it ideal for UV-selective optoelectronic applications such as photodetectors and sensors.[128,129] Although various low-dimensional ZnS nanostructures have been synthesized, systematic studies on ZnS nanostructure arrays have only recently advanced, unveiling new opportunities to exploit their unique properties.[130] Furthermore, growing research on ZnS–graphene nanocomposites highlights the synergistic interaction between the two materials, leading to improved photocatalytic and electronic performance.

4.3 Graphene/metal-based nanohybrids

Photo-corrosion represents a significant limitation to direct bandgap semiconductors like CdS (~2.4 eV), which have relatively good properties for visible spectrum light harvesting. Beyond stabilizing the photocatalyst, encapsulating CdS with graphene would help with charge separation.[131] Acting as an electron sink, graphene minimizes recombination losses and improves durability, by lowering the operating rates while light is present. The CdS/graphene systems have experienced promising CO_2 reduction rates and high quantum yields.[132]

Another layered semiconductor with better catalytic properties and hydrogen evolution properties is MoS_2.[133] When combined with graphene, MoS_2 can reduce CO_2 by facilitating charge transfer and providing extra edge sites.[134] MoS_2/graphene composites demonstrate high rates of conversion of CO_2 to CH_4 when exposed to visible light and the fact that they are hybrids ensures good interfacial contact and effective separation of photogenerated carriers.[135]

In order to solve cost issues, the incorporation of accessible non-noble metals (Ni, Co, and Cu) has emerged.[136] These metals are catalytic and have adequate proximity to graphene and

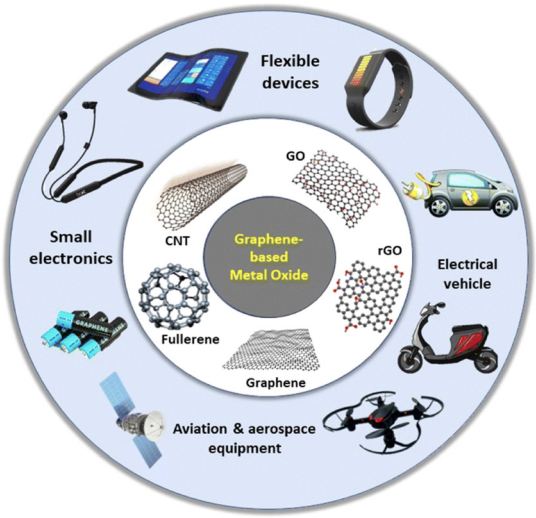

Fig. 14 Graphene/metal-based nanohybrids. Reprinted from ref. 96, copyright@2024, RSC.

increased efficiencies of electron transport pathways. Ni/graphene composites provide enhanced CO_2 adsorption and activation abilities, making them appealing candidates for photoreduction applications.[137] Co and Cu NP's help support the dynamics of charge carriers while also participating in multi-electron transfer processes.[138] In metal type nanohybrids shown in Fig. 14, graphene functions as a conductive support medium and as a functional medium to stabilize metal particles, limit aggregation, and manipulate electrical properties at the interface, thus improving photocatalytic performance.[139]

4.4 Graphene/carbon nitride and 2D/2D heterostructures

As shown in Fig. 15, 2D/2D heterostructures of graphene and other two-dimensional materials provide a new architecture to help in photocatalysis. In a layered composite format, conducive photocatalytic CO_2 conversion occurs because composites allow improved proximity, faster charge transport, and light absorption.[140]

Graphene/g-C_3N_4 2D/2D heterostructures represent a new area of interest due to their synergistic properties. g-C_3N_4 absorbs visible light and has photocatalytic activity, while graphene has solid-state conductivity and promotes charge transport.[142] Thus, a combination of these material properties provides substantial improvements to the standard photocatalytic performance observed in methane and methanol yields under simulated solar light exposure. Other two-dimensional materials such as MoS_2, WS_2, and layered double hydroxides (LDHs) have been used as van der Waals heterojunctions with graphene.[143] These heterojunctions improve charge separation with electric fields formed in-plane and overlapping conduction and/or valence bands.[144] A heterojunction of MoS_2/graphene hybrid superstructures improves CO_2 reduction reaction activity and stability because the edges of MoS_2 form catalytic sites and graphene is a very effective conductor.[145]

The very thin dimension of 2D materials generates a high surface-to-volume ratio, resulting in a greater density of exposed active sites, drastically reduces the charge diffusion distances, and has the potential to improve CO_2 and photoreduction kinetics, but facilitates coupling to light-harvesting systems like sensitizers and dyes.[146,147]

4.5 Graphene-based Z-scheme photocatalytic systems

Z-scheme systems incorporate two semiconductors to accomplish efficient charge separation while utilizing both reduction and oxidation potentials, simulating natural photosynthesis as shown in Fig. 16.[148] In the Z-scheme transistor topologies, graphene is always used as an electron mediator, allowing for fast electron transport and therefore improved charge carrier dynamics.[149] In traditional Z-scheme processes with two semiconductors, a redox mediator physically connects two semiconductors with semi-ideal band alignment and free charge movements and generates problems of low efficiencies and back reflexes.[150] For example, graphene facilitates electron transfer from g-C_3N_4 to TiO_2 pigment, so that the redox potentials stay high and the photocatalytic efficiency of the CO_2 photoreduction products improves.[151,152]

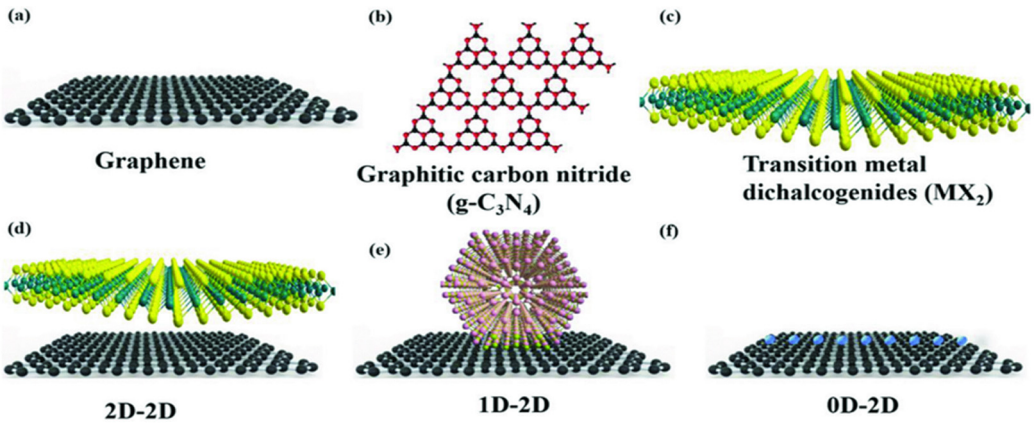

Fig. 15 Graphene-based hybrid architectures for catalysis and their heterostructures: (a) graphene, (b) g-C_3N_4, (c) transition metal dichalcogenides, (d) 2D–2D, (e) 1D–2D, and (f) 0D–2D. Reprinted from ref. 141, copyright@2019, Wiley Online Library.

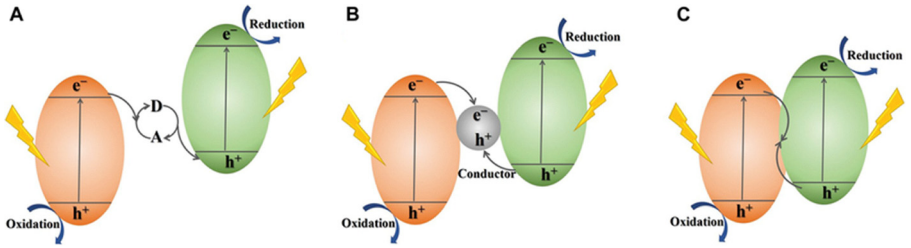

Fig. 16 Schematic of the different types of Z-scheme photocatalytic systems: (A) traditional Z-scheme photocatalytic system, (B) all-solid-state Z-scheme photocatalytic system, and (C) direct Z-scheme photocatalytic system. Reprinted from ref. 153, copyright@2024, Frontiers in Chemistry.

There have also been dual-component systems that involve graphene improving the interfacial contact, as well as reducing direct charge recombination, such as $BiVO_4$/graphene/g-C_3N_4 and CdS/graphene/$ZnIn_2S_4$. These arrangements utilize the conductive pathway of graphene in order to create direct charge flow, which enhances quantum efficiencies and product yield.[154]

In addition, heterojunctions are more structurally robust when supported with graphene allowing for greater resistance to changing environmental situations.[155] High rates of CO_2 reduction have become achievable due to the wide variety of applications humans have created for such designs, particularly under visible to solar light.[156] All and all, Z-scheme graphene-based systems are a complex photocatalytic architecture, which should promote reduction and charge recombination losses while maximizing light harvesting and redox potentials. The potential for these to scale up solar to fuel technology is exciting.[157–161]

In recent years, various other graphene-based composites have emerged as highly efficient photocatalysts for CO_2 reduction owing to their superior conductivity, large surface area, and ability to promote charge separation. A concise summary of representative systems, their photocatalytic performance, and the resulting products is presented in Table 3.

5. Mechanistic insights and charge dynamics in graphene-based photocatalytic CO_2 reduction

The rational design of graphene-based materials with enhanced photocatalytic properties necessitates some understanding of the mechanisms governing photocatalytic CO_2 reduction. The addition of graphene and its derivatives can significantly alter band structures, light harvesting efficiencies, and charge carrier dynamic behaviours.[196] In this section, we will also discuss the nature of interfaces that separate and transport charge in conjunction with graphene's contributions to improve the performance of photocatalysts, as well as the theoretical and experimental frameworks that support these operational mechanisms.[197]

5.1 Charge separation and migration at graphene interfaces

The effective production, separation, and transportation of photo-induced electron–hole pairs are key to photocatalytic efficiency. Rapid recombination of these carriers due to charge carrier motion limits the number of electrons available for reducing CO_2 on typical semiconductor photocatalysts.[198] The unique structure of graphene acts as both a mediator and an electron acceptor at the interface to eliminate this challenge.[199] Photogenerated electrons from the CB are transferred to the graphene sheet because of the energy level alignment and difference in the two Fermi levels when semiconductors such as TiO_2, ZnO, or g-C_3N_4 are combined with graphene or rGO.[200] The transfer of these electrons decreases their chance to recombine and increases their time to interact with the adsorbed CO_2 on the surface, as shown in Fig. 17.[201,202]

Moreover, the two-dimensional structure and high conductivity ($\sim 10^4$ S cm^{-1}) of graphene provide a rapid and directional pathway for charge migration.[204] This network of conductive sheets reduces the distance between separate photocatalytic nanoparticles, and therefore, facilitates a more uniform distribution of charge carriers across the surface of the catalyst and greater electron migration between adjacent particles.[205]

5.2 Synergistic roles of graphene in light absorption and carrier mobility

Even without a bandgap, pristine graphene lacks the characteristics of an intrinsic photoactive substance; nonetheless, when combined with other materials it can improve light harvesting and charge transportation capabilities in photocatalysts.[206] By limiting nanoparticle agglomeration in the composite and ultimately increasing light scattering centers throughout the composite material, graphene enhances the light absorption *via* improved light harvesting.[207]

In addition, when graphene is mixed with plasmonic metals such as Au or Ag, it will modify the optical response of the composite system.[209] The localized surface plasmon resonance (LSPR) of noble metal–graphene hybrids will lead to an enhancement in visible light absorption and induce hot electrons that may be transported to graphene and used in CO_2 reduction, as shown in (Fig. 18).[210] Graphene also significantly enhances the mobility of charge carriers. Due in large part to the delocalized π-electron system, the energy wasted when carriers migrate is minimized since it offers a fast transport path. Graphene can act as reasonably inert, solid-state electron mediators in Z-scheme photocatalytic setups, recombining

Table 3 Overview of the CO_2 photocatalytic conversion into solar fuels and value-added chemicals using the graphene-based composite photocatalysts

Composite photocatalyst	Light source	Reaction medium	Main products	Photocatalytic performance	Ref.
Graphene-WO_3 nanobelt composite	Xenon lamp, 300 W	CO_2 and gaseous H_2O	CH_4	Conversion rate: 0.89 μmol h^{-1} (after 8 h of irradiation)	162
$ZnIn_2S_4$/N-graphene	Xenon lamp (300 W)	84 mg $NaHCO_3$, 2 M H_2SO_4	CO, CH_3OH, CH_4	CH_4: 1.01 μmol h^{-1} g^{-1} CO: 2.45 μmol h^{-1} g^{-1} CH_3OH: 1.37 μmol h^{-1} g^{-1}	163
Graphene-g-C_3N_4 (15 wt%)	Daylight bulb, 15 W	CH_4	CH_4	5.87 μmol g^{-1} (after 9 hour) 2.3-fold than that for g-C_3N_4	164
Modified graphene oxide (GO)	300-Watt halogen lamp irradiation	CH_3OH	CH_3OH	Conversion rate: 0.172 μmol g^{-1} h^{-1} (six-fold higher than the pure TiO_2)	165
Cu-Nanoparticle Decorated Graphene Oxide	One-pot microwave process (2 h of visible irradiation)	$Cu(NO_3)_2{\cdot}3H_2O$ in ethylene glycol		Conversion rate: 6.84 μmol g-cat^{-1} h^{-1} (60 times higher than that for pristine GO)	166
Platinum modified rGO with TiO_2 nanotubes	Xenon lamp, 300 W		C_2H_5OH and CH_3COOH	Conversion rate: 1130 nmol h^{-1} cm^{-2}	167
Graphene derivative TiO_2	Mercury vapour lamp		Methanol, Ethanol	Ethanol production rate: 144.7 μmol g^{-1} h^{-1} at pH 11.0. Methanol production rate: 47.0 μmol g^{-1} h^{-1} at pH 4.0.	168
Noble metal nanoparticles (Pt, Pd, Ag, Au) immobilized on rGO–TiO_2	Xenon arc lamp, 500 W (6 h of light irradiation)	CO_2 and H_2O vapor	CH_4	Conversion rate: 1.70 μmol $g_{cat}{}^{-1}$	169
Graphene-supported TiO_2 nanocrystals with coexposed[110] and[115] facets (G/TiO_2-001/101)	300 W Xe arc lamp	CO_2 + H_2O	CO	70.8 mmol g^{-1} h^{-1} CO yield	170
Reduced graphene oxide (rGO)–copper oxide nanocomposites	visible light irradiation	CO_2	Methanol	Pristine CuO nanorods showed low photocatalytic activity due to fast charge-carrier recombination, producing only 175 μmol g^{-1} methanol. rGO–Cu_2O nanocomposites exhibited a five-fold improvement, yielding 862 μmol g^{-1} methanol. rGO–CuO nanocomposites achieved a seven-fold improvement, yielding 1228 μmol g^{-1} methanol.	171
GO-supported oxygen-TiO_2	Xenon arc lamp (400 nm)	CO_2 and H_2O vapor	Methane	Methane (CH_4) yield: 3.450 μmol $g_{cat}{}^{-1}$	172 2017
CuO/Cu_2O nanowire (NW) arrays grafted with reduced graphene oxide (CuO/Cu_2O NWAs@rGO)	Xenon arc lamp, 500 W	CO_2 + H_2O	CO	Enhanced CO production compared to bare CuO/Cu_2O NWAs due to slower charge recombination and efficient electron transfer through rGO nanosheets Carbon monoxide (0.31 and 0.20 mmol cm-2)	173
Pt-sensitized graphene-wrapped defect-induced blue-colored TiO_2	300 W Xenon lamp	Continuous flow-through CO_2 + H_2O	CH_4, C_2H_6	259 μmol g^{-1} CH_4, 77 μmol g^{-1} C_2H_6 (7.9% AQY; 5.2% CH_4, 2.7% C_2H_6), stable for 42 h	174
graphene oxide modified with cobalt metallated aminoporphyrin	450 W Xenon lamp	CO_2	Formic acid	Formic acid yield: 96.49 μmol in 2 h.	175
In_2O_3–rGO nanocomposites	Visible light	CO_2 + H_2O	CH_4	953.72 μmol g^{-1}	176
α-Fe_2O_3–ZnO rod/reduced graphene oxide (rGO) heterostructure	Visible light and UV-Vis light Xenon Lamp	CO_2 + H_2O	CH_3OH	Under visible light: 1.8 μmol g^{-1} h^{-1}, total 5.3 μmol g^{-1} in 3 h; under UV-vis: 3.2 μmol g^{-1} h^{-1}, total 9.7 μmol g^{-1} in 3 h; ∼10× higher than ZnO; stable (90% activity retained after 3 cycles)	177
Poly(3-hexylthiophene) nanoparticles/graphene oxide (P3HT NPs/GO)	Visible light (sunlight)	Gas-phase CO_2	CH_3OH (methanol), CH_3CHO (acetaldehyde)	CO_2-to-CH_3OH production: 3.4× higher than pristine GO; total solar fuel yield: 5.7× higher than GO; improved dispersion with SDS nearly 2× higher yield than without SDS; overall solar-to-fuel conversion efficiency 13.5× higher than GO	178
Chlorophyll-Cu/graphene (Chl-Cu/graphene)	Visible light (420 nm)	CO_2 + H_2O	C_2H_6 (only product)	68.23 μmol m^{-2} h^{-1} C_2H_6 yield; 1.26% AQE; high selectivity and stability over 18 h	179
Au–TiO_2 decorated N-doped graphene (ANGT-x, optimized ANGT2)	Xenon lamp, 300 W (l > 420 nm)	CO_2 + H_2O vapor	Methane (CH_4, highly selective)	Electron consumption rate: 742.39 μmol g^{-1} h^{-1} (for ANGT2); catalytic activity ∼4× higher than ANGT0 and ∼60× higher than binary Au–TiO_2; best reported PCO_2R rate under comparable conditions	180

Table 3 (*continued*)

Composite photocatalyst	Light source	Reaction medium	Main products	Photocatalytic performance	Ref.
rGO-grafted NiO–CeO_2 nanocomposite	Xenon lamp, 300 W	CO_2 + H_2O	Formaldehyde (HCHO)	421.09 μmol g^{-1} h^{-1} (≈ 4× higher than pristine CeO_2)	181
G-$Ti_{0.91}O_2$ hollow spheres	300 W xenon lamp	CO_2 and H_2O vapor	CO, CH_4	CO: 8.91 μmol g^{-1} h^{-1} CH_4: 1.14 μmol g^{-1} h^{-1} ~5× higher total CO_2 conversion than $Ti_{0.91}O_2$ spheres; CO dominant; enhanced charge separation, electron transfer to graphene, and photon-trapping from hollow structure	182
Cu_xO/graphene oxide (GO)/Cu-MOF (Cu-BTC) ternary composite photocathode	Xenon lamp150 W, AM 1.5 filter (100 mW cm^{-2})	Aq. electrolyte + CO_2	Ethanol, methanol and propanol	Ethanol yield: 162 μM cm^{-2} after 4 h; improved charge separation and CO_2 binding confirmed by DFT; Cu-BTC composites reported alcohol yields up to 2217 nmol h^{-1} cm^{-2} (MeOH, EtOH, PrOH)	183
RGO–CdS nanorods (0.5 wt% RGO)	Visible light, 300 W xenon lamp	CO_2 and H_2O vapor	CH_4	2.51 mmol h^{-1} g^{-1}; >10× higher than pure CdS; outperforms Pt–CdS under same conditions; RGO acts as electron acceptor/transporter, enhancing charge separation and CO_2 adsorption	184
SWCNT–TiNS (1D–2D) and SEG–TiNS (2D–2D) nanocomposites	UV (365 nm) and visible (>380 nm) light	CO_2 (water-saturated atmosphere)	CH_4	Under UV: SEG–TiNS showed up to 3.5× higher CH_4 production *vs.* TiNS, while SWCNT–TiNS showed 2× improvement. Under visible: SWCNT–TiNS showed up to 5.1× improvement, SEG–TiNS 3.7 ×, compared to TiNS. SEG–TiNS superior under UV (73.5% more CH_4 than SWCNT–TiNS), while SWCNT–TiNS superior under visible due to photosensitization.	185
Graphene–TiO_2 (G-TiO_2, 2 wt% graphene)	300 W xenon lamp	CO_2 + H_2O vapor system	CH_4, C_2H_6	C_2H_6, 16.8 μmol h^{-1} g^{-1}; CH_4, 8 μmol h^{-1} g^{-1}; solar fuel production rate is 1.7-fold of TiO_2	186
Ag NW–RGO/CdS NW (ACG-2 wt%)	Visible light, 300 W xenon lamp	H_2O (for water-splitting), H_2O/CO_2 (for CO_2 reduction)	H_2, CO, CH_4, reduced nitro-aromatic compounds	H_2: 70.6 μmol (7× higher than CG-2 wt%); CO: 3.648 μmol g^{-1}; CH_4: 1.153 μmol g^{-1}; nitro-aromatic reduction enhanced compared to CG-2 wt%	187
Au–Cu/graphene/Cu_2O (3D coaxial NW array)	Visible light, 300 W xenon lamp	CO_2 saturated H_2O	CH_3OH	18.80 ppm cm^{-2} h^{-1} methanol production rate	188
Cu_2O/RGO	Simulated solar light, 500 W xenon lamp (400 nm)	CO_2 + H_2O	CO, CH_4	Nearly 6× higher activity than optimized Cu_2O and 50× higher than Cu_2O/RuO_x after 20 h; apparent quantum yield ~0.34% at 400 nm; enhanced photocurrent and stability due to efficient charge separation and RGO protection	189
ZnO-RGO	Simulated solar light, 500 W xenon lamp	CO_2 saturated $NaHCO_3$ solution	CH_3OH	4.6 μmol h^{-1} g^{-1}; 1.7 times higher than pure ZnO	190
$Fe_2V_4O_{13}$/RGO/CdS	Visible light, 300 W xenon lamp	CO_2 and H_2O vapor	CH_4	2.3 μmol h^{-1} g^{-1}; 1.5-fold higher than $Fe_2V_4O_{13}$–CdS	191
Graphene-TiO_2	Mercury lamp (200 W)	CO_2, triethylamine vapor	CO	CO conversion rate: 1.26 μmol mg^{-1}	192
MOF-808/reduced graphene oxide	Xenon lamp	CO_2, H_2O	CO	CO conversion rate: 14.35 μmol g^{-1}	193
ZnO/N-doped reduced graphene oxide	Xenon lamp (300 W)	84 mg $NaHCO_3$, 2 M H_2SO_4	CH_3OH	CH_3OH conversion rate: 1.51 μmol h^{-1} g^{-1} (2.3 and 4.7 times higher than that of the pristine ZnO and commercial ZnO)	194 2021
RGO–P25; SEG–P25	UV light: 100 W mercury vapor lamp Visible light: 60 W daylight bulb	CO_2 and H_2O vapor	CH_4	Under UV light: −1.9 μmol m^{-2} h^{-1}, comparable to TiO_2 −8.5 μmol m^{-2} h^{-1}, 4.5 times higher than TiO_2 Under visible light: −1.3 μmol m^{-2} h^{-1}, 2.3 times higher than TiO_2 −4.0 μmol m^{-2} h^{-1}, 7.2 times higher than TiO_2	195

less energetic electrons and holes from the two different semiconductors in a selective manner, while still retaining the high redox potential of the remaining charge carriers.[13,211,212]

5.3 Experimental and theoretical investigation

A large body of experimental and theoretical evidence supports the application of graphene modifications to photocatalytic

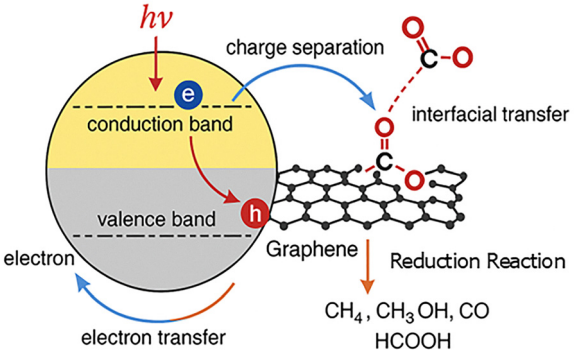

Fig. 17 Mechanistic insights in charge transfer dynamics. Reprinted from Ref. 203, copyright@2025, RSC.

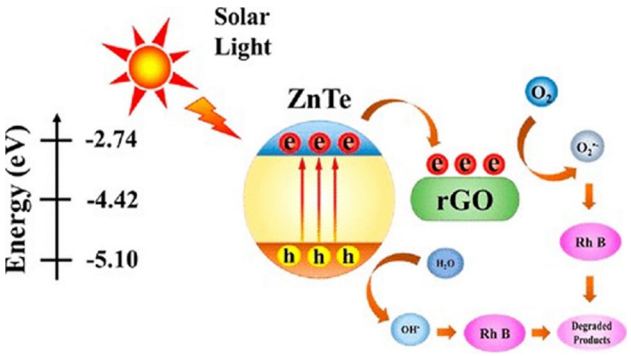

Fig. 18 Plausible mechanism of the photocatalytic degradation process of RhB containing the R–*ZT* catalyst under solar light irradiation. Reprinted from ref. 208, copyright@2022, the ACS.

reactions.[213] Charge dynamics in graphene-based photocatalysts have been assessed by the use of methods such as surface photovoltaic (SPV) measurements, electrochemical impedance spectroscopy (EIS) measurements, photoluminescence (PL) spectroscopy, and time-resolved fluorescence.[214–216]

For examples shown in Fig. 19, hybrids containing graphene often showed reduced emission intensity in the PL spectra, which indicates reduced electron–hole recombination.[218]The increased interfacial conductivity was demonstrated by EIS measurements, which generally show reduced charge-transfer resistance for graphene-based composites as compared to clean semiconductors.[219,220] Transient absorption spectroscopy (TAS) and time-correlated single-photon counting (TCSPC) offer direct insights into charge carrier lifetimes, with graphene-based materials having much increased lifetimes – often by orders of magnitude.[221,222] Surface photovoltage imaging experiments showcase better charge separation and charge carrier dispersion on graphene-modified surfaces.[223]

Modelling approaches utilizing DFT have assisted in elucidating interfacial charge transfer, modification of the band structure, and CO_2 adsorption energies.[224] DFT simulations suggest that charge transfer to heteroatom-doped graphene (for example N-doped, B-doped) exhibits higher CO_2 binding energy and far lower energy barriers for multi-electron transfer processes.[225] Coupling with graphene may better align semiconductor conduction or valence band edge with CO_2 reduction redox potentials, as simulations have indicated.[226,227]

5.4 Graphene-induced defect engineering and bandgap modulation

Defects can markedly alter the electrical properties and reactivity of graphene for both intrinsic defects and defects created during synthesis.[228] Specifically, functional groups, vacancies, Stone–Wales defects and dopants allow for effective sites for CO_2 adsorption and activation, due to their capacity to modify the band structure and introduce localized electronic states.[229,230] Defect engineering in GO or rGO opens up possibilities for bandgap tuning and reactive oxygen-bearing

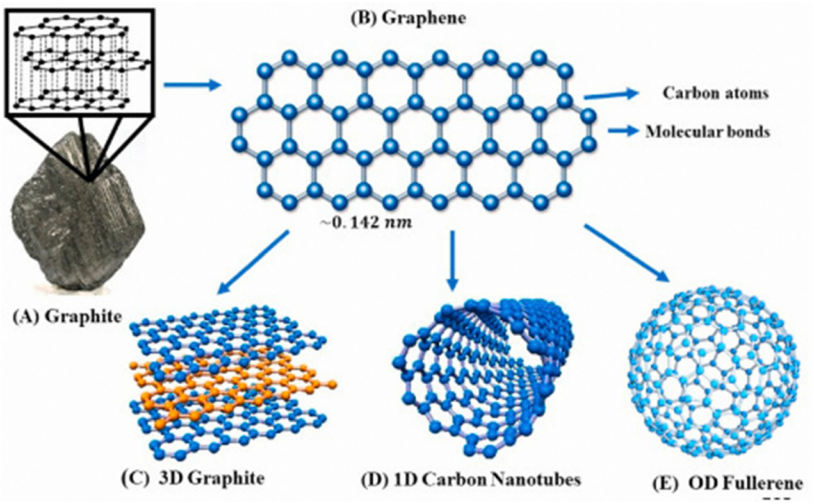

Fig. 19 Schematic of the origin and the transformation of graphite to graphene's atomic structure. The transformation process shows that graphene, a 2D basic unit of carbon, can be folded into (C) 3D graphite (D) rolled into 1D nanotubes (E) and folded into 0-D fullerene. Reprinted from ref. 217, copyright@2023, ACS.

functionalities (such as –OH, –COOH, and –C═O) that not only act as anchoring sites for the nanoparticles, but also allow for dipole and hydrogen bonding with CO_2 molecules to enhance contact of CO_2 with the reaction sites.[231,232] These defects can also be potential charge trapping sites to stabilize catalytic intermediates and extend charge separation steps.[233]

Heteroatom doping with N, S, B, or P can change the electronic density and bandgap of graphene to further improve the photocatalytic activity. For example, N-doped graphene establishes electron-rich regions which can facilitate proton-coupled electron transfer and activation of CO_2 because of the lone pairs which donate electrons to nearby carbon atom(s).[195,234] Engineering the band structure of graphene in a heterojunction is also possible with 2D/2D heterojunctions. Heterojunctions with layered materials such as MoS_2 or g-C_3N_4 provide strong interfacial interaction with few 2D materials, while spatially separating electrons and holes through the band alignments results in staggered band alignments (type-II or Z-scheme).[235,236]

Oxygen-doped graphene (GO and rGO) plays a particularly important role due to the abundance of oxygen-containing functional groups, which not only improve the dispersibility of graphene but also provide abundant active sites for anchoring semiconductor species.[237] Residual oxygen groups in rGO are reported to enhance electron transfer by serving as electron-accepting and -shuttling sites, while also inducing bandgap narrowing in semiconductor composites through chemical bonding (*e.g.*, Ti–O–C linkages), as shown in Fig. 20.[238] This leads to red-shifts in light absorption and enhanced photocatalytic performance. However, oxygen functionalities also introduce a trade-off: while they increase absorptivity and porosity, they may reduce carrier mobility by disrupting the π-network. Interestingly, graphene oxide can also act as a standalone semiconductor with a tunable bandgap, although its photoactivity is limited by instability under prolonged irradiation.

Nitrogen-doped graphene (NGR) has attracted significant attention as a superior alternative to rGO due to its ability to preserve more of the sp^2 carbon network while introducing active nitrogen sites.[240] Nitrogen atoms contribute additional π-electrons, thereby improving the electronic density of states near the Fermi level and markedly enhancing conductivity compared to rGO, as shown in Fig. 21.[241] This increased conductivity promotes efficient electron–hole separation, delays recombination, and boosts photocatalytic durability. Furthermore, different nitrogen configurations—graphitic, pyridinic, and pyrrolic—introduce distinct surface states that act as catalytic centres and improve interfacial contact with semiconductor nanoparticles, thereby strengthening photocatalyst–support interactions.

Phosphorus-doped graphene (P-G) has also shown promise, as P atoms induce semiconducting behaviour in graphene and open a tunable bandgap (up to ~2.85 eV), enabling visible-light-driven photocatalysis.[243] The incorporation of P atoms reduces defect density while enhancing the material's electronic properties. In particular, P-doping favors hydrogen evolution reactions under visible light, outperforming GO and rGO analogues in photocatalytic hydrogen generation.[244]

Sulfur doping, particularly in nitrogen–sulfur co-doped graphene quantum dots (N, S-GQDs), further extends visible-light absorption due to new surface states introduced by sulfur functionalities (C═S and S═O).[245] These dopants enable broad absorption bands in the visible region and confer sensitizing properties, allowing GQDs to act as efficient electron donors when coupled with semiconductor photocatalysts such as TiO_2.[246] The enhanced photoluminescence and surface charge properties imparted by sulfur doping strengthen the structure–activity relationship in such composites.

Taken together, these heteroatom modifications significantly broaden the photocatalytic capabilities of graphene-based materials. Oxygen doping primarily facilitates surface reactivity and bandgap modulation, nitrogen doping enhances conductivity and electron mobility, phosphorus doping introduces stable bandgap engineering with reduced defect states, and sulfur doping expands visible-light utilization. The synergy of these dopants not only improves charge separation and transport but also enables selective production of solar fuels and chemicals under tailored reaction conditions.

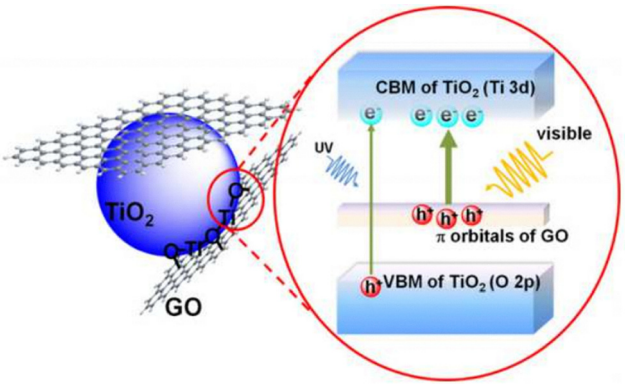

Fig. 20 Schematic of Ti–O–C chemical bonding which introduces a localized state and renders band gap narrowing. Reprinted from ref. 239, copyright@2019, Springer.

6. Influence of synthesis strategies on photocatalytic efficiency

The structural attributes of graphene-based photocatalysts chiefly determined through the synthesis approaches of the working moieties are directly related to their performance in CO_2 reduction.[247]The various approaches will affect the shape, defect density of the material, crystallinity, surface chemical properties and interfacial contact between the graphene component and the active components of the composite, all of which impact the catalytic efficiency, charge separation and light absorption.[248] This section discusses about the impact that various synthesis approaches have on the photocatalytic activity and sustainability of graphene-based materials, focusing on hydrothermal, electrochemical, photoreduction and green synthesis processes.

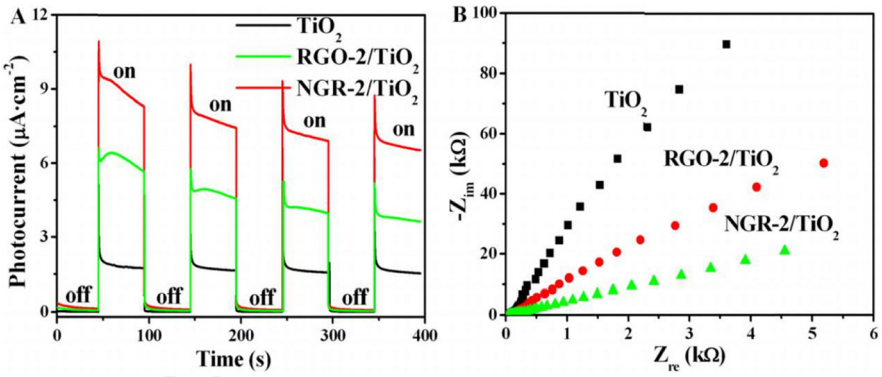

Fig. 21 (A) Transient photocurrent of TiO_2, RGO/TiO_2 and NGR/TiO_2 to chopped light irradiation. (B) Nyquist plot of the electrochemical impedance spectra for TiO_2, RGO/TiO_2 and NGR/TiO_2. Reprinted from ref. 242, copyright@2025, Elsevier.

6.1 Hydrothermal/solvothermal approach

Graphene-based nanocomposites are frequently developed by hydrothermal and solvothermal methods, which are also economic and scalable methods with the possibility of producing well-crystallized forms that may have good interfacial contact between graphene and active components.[249] During the hydrothermal/solvothermal method shown in Fig. 22, GO or rGO is readily dispersed with metal precursors in aqueous or organic solutions before heating and pressurizing a sealed autoclave.[250] Over these heating and pressurizing conditions, nucleation and growth of semiconductors or metal-oxide nanoparticles (*e.g.*, TiO_2, ZnO, and $BiVO_4$) can occur directly on the peeled-off GO or rGO sheets. Greater interfacial coupling is also known to improve photocatalytic CO_2 reduction *via* better electron transfer and suppressing electron–hole recombination.

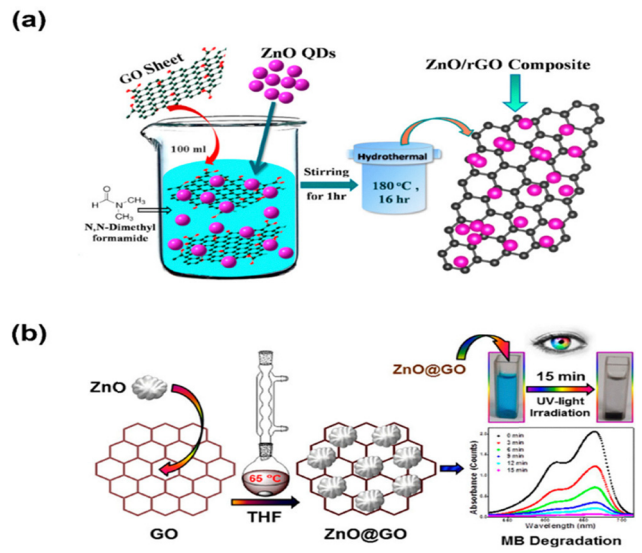

Fig. 22 Synthesis of graphene based hybrid material: (a) hydrothermal synthesis of ZnO/GO nanocomposites (reprinted from ref. 251, copyright@2016, Elsevier) and (b) solvothermal synthesis of ZnO/GO nanocomposites (reprinted from ref. 252, copyright@2024, MDPI).

Fine tunings of synthesis conditions have the potential to induce vast differences in the catalytic activity of hydrothermally synthesized materials. A good example is how different reaction temperatures alter the crystallinity of the precipitated nanoparticles. Elevated temperatures often help promote the crystallinity or order of solid, thus minimizing structural defects that act as recombination sites for charge carriers, whilst also increasing the lifetime of charge carriers. This outcome was associated with ZnO–graphene hybrids, where increased CO_2-to-CO conversion efficiencies and crystallinity resulted from elevating the hydrothermal temperature from 120 °C to 180 °C, and several crystallinity defects resulted in reduced conversion efficiencies. Conversely, if the temperature is too high, charge carriers can act as glues between nanoparticles resulting in agglomeration, which reduces both the surface area and number of active sites in a sample, which can subsequently decrease CO_2 adsorption ability. Time is also critical; longer hydrothermal times frequently enhance stability and increase the relative size and homogeneity of nanoparticles whilst promoting better interactions in the hybrid structure of nanoparticle-graphene. However, prolonged growth also reduces the defect density, which may limit the availability of catalytically active sites. In contrast, shorter reaction times can generate smaller nanoparticles with higher defect density, potentially increasing the catalytic activity by creating additional active centers, albeit at the expense of structural stability.

The pH of the precursor solution and the concentration of metal salts are just as important as temperature and time for nucleation and growth of the nanoparticles. On graphene, we typically produced smaller, more evenly dispersed nanoparticles from faster nucleation rates at higher pH. This is important for the effective electron transport of the composite. The precursor concentration affects the loading density of the nanoparticles: mid-range concentrations evenly distribute the loaded nanoparticles and help maintain graphene conductivity and improve electron–hole separation, while extreme concentrations can lead to nanoparticle collisions with one another, blocking graphene surfaces and limiting charge mobility. The ultimate impact on photocatalytic activity, photon absorption and CO_2 reduction rate is dependent on the balance of factors

of crystallinity, defect density, surface chemistry and interfacial contact – all determined collectively from a balance of these interdependent factors.[253]

6.2 Electrochemical and photoreduction methods

For producing graphene-based photocatalysts, both electrochemical and photoreduction technologies have become attractive alternatives to conventional chemical reduction. As they can be applied under relatively mild conditions, and because they offer precise control of both the level of reduction and nanoparticle deposition, both methods are considered to be ''greener'' since they do not use harsh reducing chemicals. For these reasons, they are suitable for making composites with electrical and structural properties, which can be tuned to directly affect their efficiency for photocatalytic CO_2 reduction.

Electrochemical reduction involves the application of an electrical bias to GO films or dispersions in an electrolyte medium, removing oxygen functional groups while partially reforming sp^2-hybridized carbon networks.[254] The extent of reduction is directly linked to the applied potential, reduction time, and electrolyte composition.[255] GO deoxygenation accelerates with applied voltage; the higher the applied voltage, the greater the extent of deoxygenation, increasing electrical conductivity and enabling rapid electron transfer across rGO films. However, excessive reduction may strip too many oxygenated groups from the rGO, leading to a decrease in surface polarity and the number of CO_2 adsorption sites, marking a negative effect on catalytic selectivity. The reduction duration is equally important in rGO production: short reduction times partially yield rGOs with a predominance of oxygen functionalities that subsequently act as anchoring sites for metal nanoparticles, while long reduction times increase conductivity, but decrease oxidation and thus limit surface reactivity.[256] As the ionic strength and metal cation presence can regulate nanoparticle nucleation and dispersion, the electrolyte's composition can also influence this process. When noble metals (Ag, Au, and Pt) or TiO_2 are deposited on rGO substrates by electrochemical reduction, for example, there is a close interfacial contact, which aids in effective electron transmission and better charge separation at the graphene–semiconductor interface.

However, photoreduction is a process that makes use of light irradiation (typically UV or visible light) along with appropriate sacrificial agents (for example, ethanol, methanol, or other organic donors) to reduce GO or reduce metal ions to graphene sheets in parallel to reducing GO. This is advantageous because it delivered a nanohybrid where there was a clean surface free from any (chemical) residual, unlike traditional chemical reduction routes. The parameters of photoreduction that influence it include: (1) the wavelength of light and the intensity of light; (2) the time of illumination using the light; and (3) the concentration of sacrificial agent present. Short-wavelength UV light gives high-energy photons that can drive highly efficacious GO reduction and rapid nanoparticle nucleation, while visible-light-assisted photoreduction is greener and more amenable to scale up. Long illumination times will likely enhance the level of reduction and nanoparticle loading; however, excessive illumination can result in particle overgrowth or photothermal agglomeration. Additionally, the sacrificial agent concentration also plays a role: moderate concentrations will facilitate the efficient transfer of photogenically generated electrons to GO or metal precursors, and high concentrations will result in either incomplete reductions or residual by-products that may passivate catalytic sites.

Electrochemical and photoreduction techniques are most effective when creating nanohybrids with uniformly dispersed nanoparticles exhibiting good interfacial contact and tunable surface chemistry. These characteristics promote charge transfer efficiency, increase carrier lifetimes, and provide large active surface sites for the adsorption and activation of CO_2, all of which in turn have a direct influence on the catalytic efficiency. Additionally, these techniques produce low energy and less toxic by-products while allowing for nominally room- to low-temperature reactions, benefiting sustainability goals for the scalable production of graphene-based photocatalysts.[257]

6.3 Green synthesis and sustainability concern

Due to growing emphasis on green chemistry, green synthesis protocols for graphene-based photocatalysts have gained significant attention.[258] With regard to conventional protocols that occasionally employ toxic solvents, high redox agents or high energy requirements, green protocols involve non-toxic solvents, biological redox agents or energy-saving protocols such as microwave-assisted or mechanochemical syntheses. The new technologies both minimize environmental effects and offer new surface functionalities that enhance photocatalytic CO_2 reduction.[259]

One of the most frequently adopted green methods is biogenic and plant-extract-mediated reduction. Plant-derived, fungus-derived, or bacterial extracts comprise polyphenols, flavonoids, alkaloids and sugars that serve both as reducing and stabilizing agents while converting GO to rGO and depositing metal nanoparticles. The composition of the extracts directly affects catalytic properties. Polyphenol–laden extracts improve the incorporation of the surface graphene's oxygenated functional groups, increasing hydrophilicity and CO_2 adsorption ability. Flavonoids and proteins, however, may act as capping agents, decrease nanoparticle size and improve dispersion.[260]

Microwave-assisted synthesis is another sustainable approach, where precursors are fairly uniformly heated quickly, and the time of reaction and energy consumption is reduced significantly *versus* traditional hydrothermal processing. The microwave power and exposure time will greatly determine the end material properties. In general, higher microwave power leads to better crystallinity and interfacial coupling, by promoting a faster reduction of GO and nucleation of metal/semiconductor nanoparticles. Extreme microwave power or excessive irradiation times can cause uncontrolled growth or agglomeration of nanoparticles, decrease the active surface area and affect mass transfer. With that stated, optimal microwave parameter manipulation allows the creation of highly porous nanocomposites with controlled shapes, large surface areas and enhanced light absorption efficiency.

Mechanochemical (solvent-free) synthesis is another environmentally friendly method that does not require an organic solvent. In the mechanochemical process, graphene sheets and catalyst precursors are closely combined by mechanical forces, including ball milling. The choices in milling speed, duration of milling, and ball-to-powder mixing ratio will directly affect the surface roughness, defects, and anchoring of nanoparticles on graphene. For example, in terms of CO_2 adsorption or electron–hole separation, short or low energy-modified milling may create mild defects, allowing for better homogenous dispersion of catalyst in the graphene encapsulated sample. In contrast, large defects created by long milling time (or high energy) can serve as charge recombination sites, reducing the overall catalytic activity of the catalyst. Therefore, optimization is required in order to properly assess the trade-off between the disadvantage of deterioration of structural integrity, and the opportunity to engineer better defects from persistent mill.

Taken collectively, green synthesis methods offer benefits that are considerable in terms of scalability and sustainability and options for tuning the electrical and structural properties of graphene-based photocatalysts, as shown in Fig. 23. Often, they lead to composites with lower crystallinity and more heterogeneity than conventional hydrothermal or chemical methods, which can detract from long-term stability and reproducibility. Therefore, future studies should focus on optimizing these methods for green chemistry and catalysis, perhaps allowing controlled parameter tuning and hybridization, such as biogenic reduction followed by microwave irradiation.[261]

6.4 Morphological tuning and surface area control

The catalytic efficiency of graphene-based photocatalysts is typically determined by controlling the morphology and surface design rather than the selection of the synthesis method.[263] The morphological parameters of the composite material, which contribute to photocatalytic efficiency through their influence on light absorption, charge separation, kinetics of surface reaction and CO_2 adsorption are equally as important as the innate electrical properties of the material.[264] Therefore, it is progressively more common to use rational modification of morphology when seeking to optimize catalytic efficiencies.

The finest strategy to produce a 3D graphene material is to produce it in the form of hydrogels, foams or aerogels. These are composite structures usually produced *via* hydrothermal self-assembly or freeze-drying, yielding connected porous networks comprising extremely high porosity and large surface areas.[265] Not only does increased porosity increase light exposure into the catalyst matrix and mass transfer of the CO_2 molecules to/from the active site, but increased porosity also increases active sites due to the increased surface area. For example, the size distribution of pores will be affected by the rate at which it is frozen. Rapid freezing yields small closed holes with potential accessibility issues, while slow freeze-drying creates larger interconnecting pores, which can be beneficial for gas diffusion. Thus, this parameter can directly affect the kinetics of CO_2 adsorption and reduction.

The size and spatial distribution of nanoparticles on graphene supports are important factors. During synthesis, the kinetics of nucleation, the use of surfactants or templates, and the concentration of precursors can be varied and achieve morphological control. Smaller and more uniformly dispersed particles form more catalytically active sites and smaller distance of electron transport channels. However, overcrowding of particles from excessive nucleation can reduce graphene's conductivity and disrupt charge mobility. However, larger nanoparticles can decrease the density of surface-active sites while promoting crystallinity. Producing a suitable morphology will require controlling the syntheses conditions in such a way to find a suitable balance between exposure of active surface sites and the efficiency of charge separation.

Morphological modification also depends upon defect engineering. Localized states that act as charge-trapping or catalytic sites are added to graphene's band structure when structural defects such as vacancies, edge sites and even heteroatom dopants (N, S, and B) are embedded (*i.e.*, with an atomic localization).[266] Because defects modified during the synthesis improve CO_2 adsorption *via* more significant binding interactions with

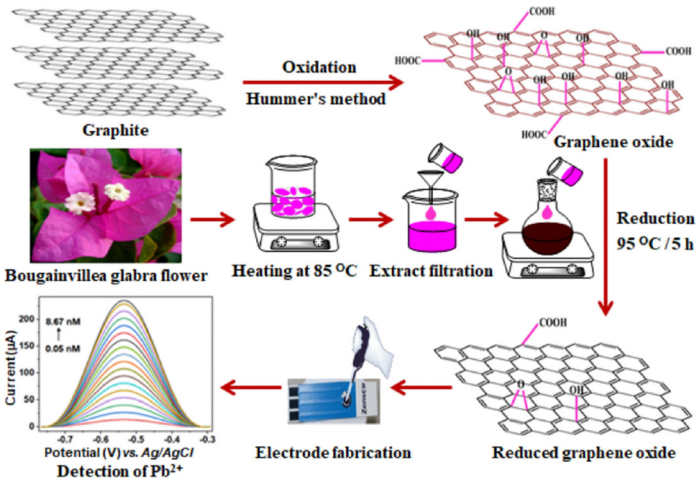

Fig. 23 Green preparation method of rGO. Reprinted from ref. 262, copyright@2025, Springer.

intermediates such as CO_2^- as formed and adsorbed at these sites, defects also help morphology-based modification. Defects must be controlled since stability might be compromised and non-radiative recombination could be enhanced if defect densities are too high. For example, nitrogen-doped graphene aerogels can exhibit increased selectivity to the production of CO by stabilizing COOH intermediates, but too much nitrogen-doping can lead to the distortion of the carbon lattice structure, which can reduce conductivity.

Finally, hierarchical and mesoporous structures enhance the photocatalytic performance by combining mesopores (to provide a greater active surface area) and macropores (for mass transfer). Template-assisted synthesis allows precise control of pore size and connectivity. The surfactant/template-to-precursor ratio is important; if too little surfactant is used, the porous structure may partially collapse, while more surfactant loading typically adds to the pore volume and surface area. The use of morphological control mechanisms provides the following synergistic balance of surface area, mass transport and charge transfer dynamics.

Surface engineering and morphological tuning are successful strategies for increasing photocatalytic CO_2 reduction capability in graphene-based composites, as shown in Fig. 24.[268] From careful manipulation of physical features (*i.e.*, pore shape, nanoparticle size and dispersion, and defect density), it is possible to optimize light harvesting, facilitate charge separation, and uncover a large number of catalytic sites. The strategies we have proposed help to bridge the gap between material development and functional performance (Table 4).

7. Photocatalytic performance evaluation

7.1 Experimental conditions and reactor configurations

The evaluation of photocatalytic performance requires standardized and reproducible experimental setups. The three main reactor configurations employed are slurry reactors, flat-panel reactors, and microreactors, each providing distinct benefits for light distribution and reactant flow. To ensure comparability, parameters such as light intensity (W m^{-2}), irradiation wavelength, CO_2 pressure and flow rate and reaction temperature must be carefully controlled.[282] For instance, slurry reactors with simulated solar light (AM 1.5G, 100 mW cm^{-2}) have been widely used, while microreactors allow higher precision with CO_2 pressures up to 2 bar and light intensities ranging from 50 to 150 mW cm^{-2}. The use of monochromatic LEDs (420–650 nm) in some studies enables direct correlation between catalyst absorption and activity, providing more detailed insights into charge transfer mechanisms.

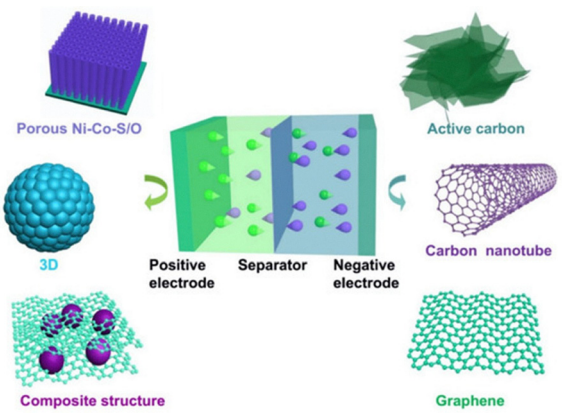

Fig. 24 Taking advantage of graphene's surface area for advanced applications. Reprinted from ref. 267, copyright@2025, MDPI.

7.2 Effect of CO_2 pressure, light source, and co-catalysts

Photocatalytic activity exhibits high sensitivity to external operating conditions. Increasing CO_2 pressure enhances reactant solubility and adsorption, leading to higher yields.[283] For example, graphene–TiO_2 composites achieved a CO production rate of 120 μmol g^{-1} h^{-1} at 1 atm CO_2, which increased to 210 μmol g^{-1} h^{-1} when the pressure was increased to 3 atm. Similarly, the choice of light source strongly influences activity: visible light irradiation ($\lambda > 420$ nm, 300 mW cm^{-2}) resulted in a 2.3-fold higher CH_4 yield for N-doped graphene/g-C_3N_4 compared to UV-only excitation. The addition of co-catalysts such as Pt, Cu, or Ni facilitates electron trapping and catalytic site formation. For instance, Pt-decorated graphene–ZnO composites exhibited an AQE of 6.2% under 365 nm irradiation, significantly higher than that of the bare composite (2.8%).

7.3 Performance metrics: its yield, selectivity and quantum efficiency

The primary performance indicators for CO_2 photoreduction include product yield (μmol g^{-1} h^{-1}), product selectivity (%), apparent quantum efficiency (AQE), and solar-to-fuel efficiency (STF).[284] Recent reports have demonstrated that graphene-based hybrids significantly outperform conventional photocatalysts.[258] For example, graphene–Cu_2O systems achieved a CO yield of 320 μmol g^{-1} h^{-1} with 82% selectivity under AM 1.5G illumination (100 mW cm^{-2}), while TiO_2 under identical conditions produced only 75 μmol g^{-1} h^{-1} with 45% selectivity. Similarly, graphene/g-C_3N_4 composites delivered CH_4 yields of 210 μmol g^{-1} h^{-1} with an AQE value of 5–8%, whereas pristine g-C_3N_4 typically showed $<2\%$ AQE. Reaction profiles are routinely characterized *via* gas chromatography (GC) for gaseous products and high-performance liquid chromatography (HPLC) for liquid intermediates.

7.4 Benchmarking with conventional and other advanced photocatalysts

Systematic benchmarking against conventional and advanced photocatalysts provides quantitative insights into the role of graphene.[285] For instance, under identical AM 1.5G conditions, graphene–perovskite composites achieved CO_2 conversion rates of 410 μmol g^{-1} h^{-1} with 85% CO selectivity and stability exceeding 120 h, compared to bare perovskites, which exhibited only 160 μmol g^{-1} h^{-1} with 62% selectivity. Likewise, graphene-modified ZnO maintained stable activity over 100 h, while pure

Table 4 Summary of synthesis methods and their impact on catalytic properties

SN	Synthesis method	Key parameter	Effect on material properties	Impact on CO_2 photocatalysis	Ref.
1	Hydrothermal/ solvothermal	Temperature	Higher crystallinity at elevated temperature; excessive heating causes nanoparticle aggregation and surface area loss	Improves charge carrier lifetime; excessive temperature reduces CO_2 adsorption	269
2	Hydrothermal/ solvothermal	Reaction time	Longer times → larger particles, lower defect density; shorter times → smaller particles, higher defect density	Balances stability and catalytic site density	270
3	Hydrothermal/ solvothermal	pH/precursor concentration	Controls nucleation density and nanoparticle dispersion on graphene	Enhances interfacial contact and electron transfer	271
4	Electrochemical reduction	Applied potential	Higher voltage improves conductivity but may reduce surface oxygen groups	Improves electron mobility but may lower CO_2 binding	272
5	Electrochemical reduction	Electrolyte composition	Ionic strength and cations influence nanoparticle deposition density and distribution	Better nanoparticle anchoring, enhanced interfacial charge separation	273
6	Photoreduction	Light wavelength and intensity	UV enables fast GO reduction; visible-light more sustainable but slower	Generates clean-surface composites with high electron transfer	274
7	Photoreduction	Sacrificial agent concentration	Moderate levels promote efficient reduction; excess may leave residues and passivate sites	Affects nanoparticle loading and catalytic efficiency	275
8	Green synthesis (biogenic)	Extract composition	Polyphenols, flavonoids add functional groups enhancing CO_2 adsorption and selectivity	Improves selectivity and CO_2 affinity; variability limits reproducibility	276
9	Green synthesis (microwave-assisted)	Microwave power and duration	Rapid, uniform heating improves crystallinity; excessive power causes agglomeration	Reduces reaction time and energy input; optimized power enhances porosity and activity	277
10	Green synthesis (mechanochemical)	Milling speed/ time	Creates defects and dispersion; excessive milling may cause too many recombination centres	Enhances CO_2 adsorption *via* defects; excessive defects cause recombination losses	278
11	Morphological tuning	Freeze-drying rate	Slow rate → larger pores, better diffusion; fast rate → smaller, closed pores	Enhances mass transport and light penetration	279
12	Morphological Tuning	Surfactant/ template ratio	Controls mesopore volume, active surface exposure	Increases active surface area and catalytic site exposure	280
13	Defect engineering	Dopant concentration	Introduces localized charge-trapping sites; excess doping distorts lattice, lowers conductivity	Stabilizes intermediates and boosts selectivity; excess defects hinder performance	281

ZnO lost 40% of its activity within 30 h. Statistical analysis and recent studies reveal consistent trends: (i) graphene incorporation enhances quantum efficiencies from 1–3% to 5–12%; (ii) CO_2 conversion rates increase by 2–5 folds relative to pristine semiconductors; and (iii) selectivity toward CO and CH_4 improves by 20–40%. These results underscore the importance of graphene as an electron mediator and structural stabilizer, establishing reliable structure–activity relationships for future catalyst design, as shown in Fig. 25.

8. Challenges and limitations

8.1 Stability and recyclability of graphene-based catalysts

Extended use of graphene-based photocatalysts often causes oxidation, mechanical delamination or photodegradation. The examination of recyclability calls for stability tests involving several photocatalytic cycles and extended illumination. Protective coverings or core–shell construction could help to reduce degradation issues.

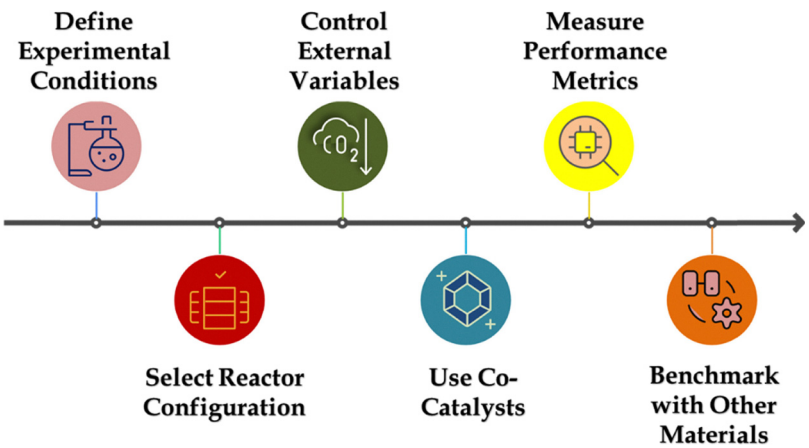

Fig. 25 Experimental setup and performance evaluation of graphene.

8.2 Scale-up and cost-effectiveness

The commercial deployment of these materials faces challenges because of large-scale synthesis difficulties and uniformity problems and high production costs despite positive lab-scale results. The development of continuous hydrothermal synthesis and roll-to-roll graphene film production techniques represents current research directions for scalability.[286] The evaluation of economic viability requires a balance between material costs and energy consumption and catalyst durability.

8.3 Standardization of testing protocols

The current differences in testing methods produce results that are both inconsistent and non-comparable between different research groups. International consortia and standard setting organizations are promoting uniform approaches, which include catalyst pre-treatment and analytical instrument calibration and error reporting.

8.4 Toxicity and environmental impact of nanomaterials

Graphene-based nanomaterials (GBNs) have been developed with the purpose of photocatalytically reducing CO_2 emissions, implying that GBNs could have a large positive impact on the environment; however, their potential health and environmental risks must be considered. Several studies have reported that GO and rGO cause mammalian cell oxidative stress, membrane damage and inflammation depending on their surface chemistry, size, and dose. In aquatic ecosystems, GBNs have been shown to interact with microorganisms, algae, and fish in ways that impact growth, reproduction, and metabolism, which raises ecotoxicological concerns. Chronic exposure to GO has been linked to diminished algal primary productivity with accumulated discharge of GO in higher trophic levels. In addition, with GBN persistence in soil and water running the risk of unknown cumulative effects, pathways for degradation such as photodegradation, microbial breakdown, and oxidative transformation are only understood in part.[287]

In response to these concerns, regulatory groups have started to take action. The European Chemicals Agency (ECHA) and the U.S. Environmental Protection Agency (EPA) have stressed that nanomaterial safety evaluations and life-cycle assessments of graphene-based materials should be nano-specific. However, the regulatory environment is still evolving, and very few regulations established have standardized protocols for toxicity testing, disposal, and risk assessment. Hence, when considering the safety of graphene nanomaterials in photocatalytic technologies, future studies must prioritize systematic research on environmental fate and bioaccumulation potential, as well as implementation of safe-by-design practices, as shown in Fig. 26.

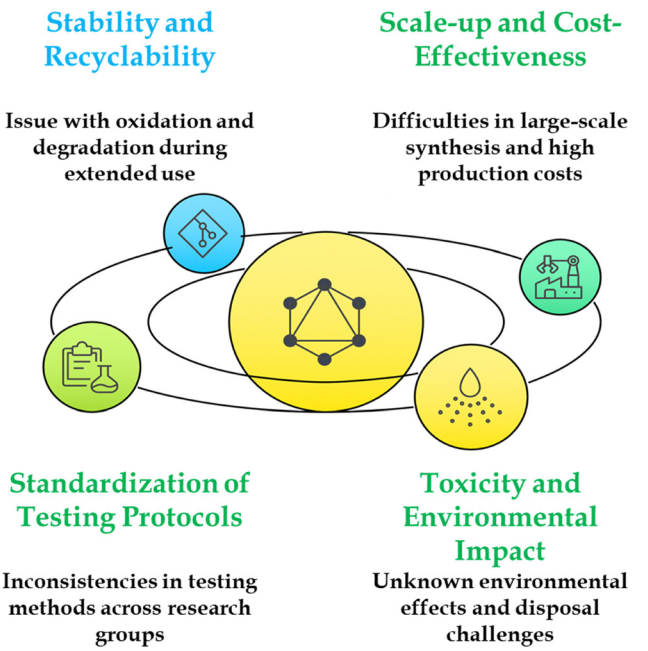

Fig. 26 Overcoming challenges in the graphene-based catalysts for CO_2 reduction.

9. Recent advances and emerging trends

9.1 Machine learning and AI in photocatalyst design

Machine learning (ML) algorithms, such as random forests and neural networks, are being trained on databases of photocatalytic performance to predict new material combinations with high efficiency. These tools accelerate discovery cycles and reduce experimental workload by identifying key descriptors for performance.

9.2 Single-atom catalysts (SACs) and defect engineering

SACs doped into the lattice of graphene or anchored on it provide customized electronic environments and optimized atomic efficiency.[288] Especially for multi-electron reduction pathways, these active sites exhibit high turnover frequencies (TOFs) and selectivity. By improving reactivity and establishing anchoring sites, defect engineering enhances SACs.

9.3 Hybrid systems: graphene with MOFs, COFs, and perovskites

The combination of graphene with MOFs, and COFs produces hybrid systems that enhance the stability and conductivity of graphene along with functionality and porosity of MOFs and COFs. Further, the hybrid perovskites-graphene materials show the superior optoelectronic properties compared to perovskites alone. The CO_2 photoreduction process benefits from these combinations of hybrid materials because they create multiphase catalytic pathways and synergistic charge separation mechanisms.

9.4 Photocatalysis under visible and near-infrared light

The spectrum needs to be made more usable for solar applications. Graphene-based composites are being designed to absorb in the visible and near-infrared spectra by using doping techniques, plasmonic coupling, or upconversion. This increases the solar-to-fuel conversion rates and enables the effective harvesting of low-energy photons.

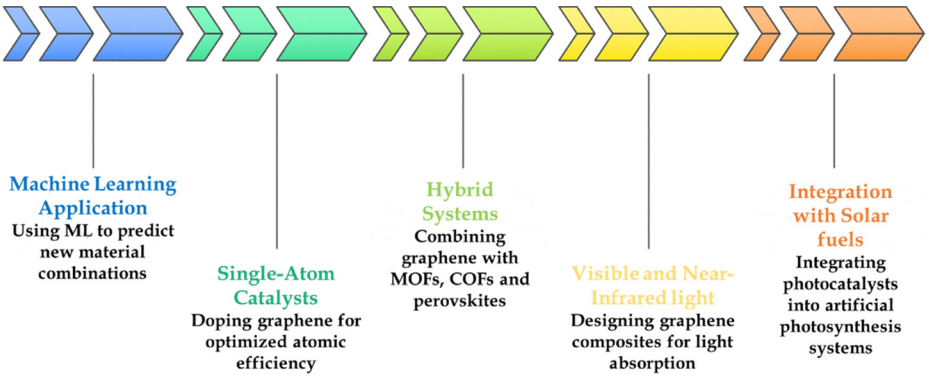

Fig. 27 Advances in photocatalysis in CO_2 reduction.

9.5 Integration with solar fuels and artificial photosynthesis systems

The development of artificial photosynthesis approaches nears completion through the integration of graphene-based photocatalysts into the complete system that includes photoanodes, cathodes and membrane separators. The integrated platforms enable sustainable carbon-neutral energy cycles through direct fuel production of methane or methanol from CO_2 and water by using sunlight, as shown in Fig. 27.[289]

10. Future perspectives and roadmap

10.1 Research gaps and new directions

The field of nanotechnology faces ongoing challenges regarding charge dynamics at the nanoscale and material stability and multifunctionality. The main research directions for the future should focus on high-throughput screening and sophisticated *in situ* characterization tools and machine learning for guided material discovery.

10.2 Toward commercial-scale CO_2 photoreduction

The advancement of technologies beyond the laboratory settings requires pilot-scale studies to demonstrate economic viability, dependability and integration with CO_2 capture units. The validation of real-world performance and technology scaling requires essential collaboration between academic institutions and industrial partners and government officials.[290]

10.3 Policy, funding, and interdisciplinary collaborations

The advancement of graphene research depends on the public and private funding initiatives, which enable laboratory discoveries to become deployable technologies. Systemic innovation will emerge from interdisciplinary partnerships between materials science and chemical engineering and environmental policy and economics researchers.

10.4 Vision for graphene-based nanomaterials in climate solutions

Graphene-based photocatalysts present a viable route for the sustainable use of CO_2. These materials can make a substantial contribution to climate mitigation by utilizing solar energy to transform greenhouse gases into useful fuels and chemicals. To achieve a carbon-neutral future, next-generation graphene hybrids and their integration into integrated energy systems will be essential as shown in Fig. 28.[291]

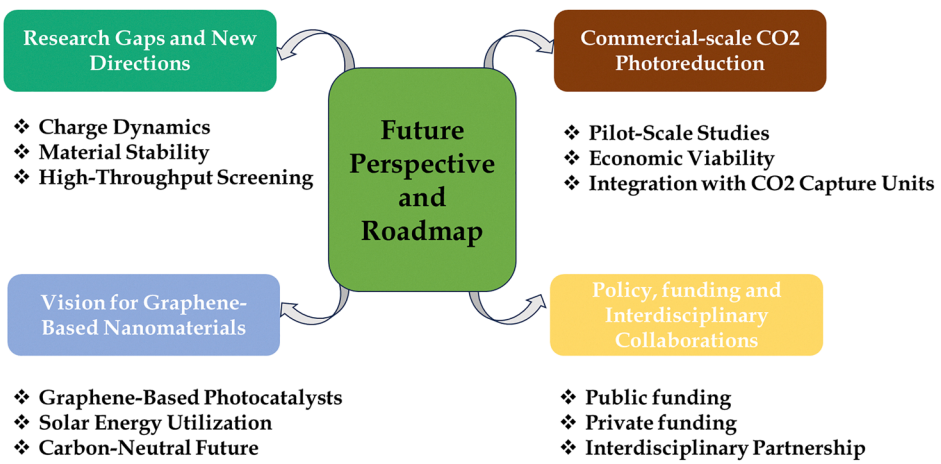

Fig. 28 Future perspective and roadmap of nanotechnology for CO_2 reduction.

11. Conclusion

Photocatalytic carbon dioxide (CO_2) reduction provides a viable pathway toward sustainable energy conversion and carbon management; however, challenges with low efficiency, poor selectivity and limited stability will continue to hinder the commercialization of photocatalytic CO_2 systems. Recent advances in the field of graphene-based nanomaterials demonstrate that their remarkable capabilities (high surface area, increasing conductivity, tunable chemistry and electron mediators) can resolve many of these impediments. The incorporation of graphene into semiconductor, metal oxide, metal and carbon nitride systems has provided significant enhancements in light absorption, charge separation and inference stabilization of key intermediates during additional reactions and resultantly increased yields of CO_2 in the form of CO, CH_4, CH_3OH and HCOOH. Further advances including bandgap, Z-scheme, plasmonic enhancements and surface functionalization have illustrated the flexibility of graphene as a co-catalyst to tune the selectivity of CO_2 photoreduction, as well as to serve as a structural platform.

However, there are still major challenges to overcome. Stability through long-term operation, scalability of synthesis pathways and the footprint of produced graphene on large scales are important factors that need to be addressed. Furthermore, although several reviews focus on model systems and laboratory conditions, our implementation of systems into commercial solar-driven reactors remains limited. As such, the research needed to solve these technical issues will require the integration of several techniques, rational engineering of interfaces, precise control over heteroatom doping and the appropriate hybridization with metals and semiconductors, such that efficiency and selectivity can be achieved at scale.

Looking forward, the combination of emerging technologies such as single-atom catalysis, machine learning-assisted catalyst design and green synthesis routes offers new opportunities for tailoring graphene-based systems toward high-performance CO_2 reduction. The synergistic integration of experimental and theoretical insights will be critical to unraveling complex reaction mechanisms and guiding the rational design of next-generation photocatalysts. With continued innovation, graphene-based nanomaterials hold immense potential to accelerate the realization of efficient, scalable and sustainable CO_2-to-fuel conversion technologies, bridging the gap between laboratory success and practical applications.

Author contributions

Abhishek R. Patel: writing – original draft & editing; Anas D. Fazal: writing – original draft & editing; Trupti D. Solanky: writing – original draft; Subhendu Dhibar: writing – original draft; Sumit Kumar: writing – original draft, funding acquisition, resources, supervision; and Sumit Kumar Panja: writing – original draft, funding acquisition, resources, supervision.

Conflicts of interest

There are no conflicts to declare. The authors declare no competing financial interests.

Data availability

No primary research results, software or code have been included and no new data were generated or analysed as part of this review.

Acknowledgements

Abhishek, Anas and Trupti thank the Government of Gujarat for financial support under the SHODH fellowship (File No. KCG/SHODH/2023-24/202301737, KCG/SHODH/2023-24/2022011739 and KCG/SHODH/2023-24/202301735). SKP acknowledges the Tarsadia Institute of Chemical Science, Uka Tarsadia University, Surat-394350, Gujarat, India, for providing the infrastructure and instrument facilities.

References

1 M. Kabir, *et al.*, Climate change due to increasing concentration of carbon dioxide and its impacts on environment in 21st century; a mini review, *J. King Saud Univ., Sci.*, 2023, **35**, 102693.
2 F. S. Islam, Clean coal technology: the solution to global warming by reducing the emission of carbon dioxide and methane, *Am. J. Smart Technol. Solutions*, 2025, **4**, 8.
3 D. Cesar Carrascal-Hernández, C. D. Grande-Tovar, M. Mendez-Lopez, D. Insuasty, S. García-Freites, M. Sanjuan and E. Márquez, CO_2 Capture: A Comprehensive Review and Bibliometric Analysis of Scalable Materials and Sustainable Solutions, *Molecules*, 2025, **30**, 5634.
4 R. Naz and M. Tahir, Recent Developments in Metal-free Materials for Photocatalytic and Electrocatalytic Carbon Dioxide Conversion into Value Added Products, *Energy Fuels*, 2025, **39**, 6127.
5 L.-L. Wu, L.-Q. Yang, W.-X. Liu, T.-Y. Hang and X.-F. Yang, Research progress on photocatalysts for CO_2 conversion to liquid products, *Rare Met.*, 2025, **44**, 4411.
6 M. Gholami and R. Sedghi, *Graphene-Based Photocatalysts for Hydrogen Production and Environmental Remediation*, Springer, 2024, vol. 219, pp. 535–562.
7 H. Liu, M. Yu, X. Tong, Q. Wang and M. Chen, High temperature solid oxide electrolysis for green hydrogen production, *Chem. Rev.*, 2024, **124**, 10509.
8 D. M. H. Pham and R. Khaliullin, *New and Traditional Density Functional Theory Methods for Unveiling Mechanisms of Green Chemistry Processes*, 2025.
9 F. Zhang, J. Liu, L. Hu and C. Guo, Recent Progress of Three-Dimensional Graphene-Based Composites for Photocatalysis, *Gels*, 2024, **10**, 626.

10 H. Khan, Graphene based semiconductor oxide photocatalysts for photocatalytic hydrogen (H_2) production, a review, *Int. J. Hydrogen Energy*, 2024, **84**, 356.
11 M. R. A. Foisal and A. B. Imran, *Graphene-Based Photocatalysts for Hydrogen Production and Environmental Remediation*, Springer, 2024, pp. 499–534.
12 J. Low, J. Yu and W. Ho, Graphene-based photocatalysts for CO_2 reduction to solar fuel, *J. Phys. Chem. Lett.*, 2015, **6**, 4244.
13 Y.-H. Chen, J.-K. Ye, Y.-J. Chang, T.-W. Liu, Y.-H. Chuang, W.-R. Liu, S.-H. Liu and Y.-C. Pu, Mechanisms behind photocatalytic CO_2 reduction by $CsPbBr_3$ perovskite-graphene-based nanoheterostructures, *Appl. Catal., B*, 2021, **284**, 119751.
14 A. Sewnet, M. Abebe, P. Asaithambi and E. Alemayehu, Visible-light-driven g-C_3N_4/TiO_2 based heterojunction nanocomposites for photocatalytic degradation of organic dyes in wastewater: a review, *Air, Soil Water Res.*, 2022, **15**, 23.
15 S. B. Nehru, N. Perumal and Y. P. Subbarayalu, Sustainable water treatment: synthesis and characterization of g-C_3N_5/$NiCo_2S_4$ heterojunction nanocomposite for efficient visible light-induced degradation of highly hazardous organic pollutants, *J. Water Process Eng.*, 2025, **73**, 107712.
16 P. Kyokunzire, G. Jeong, S. Y. Shin, H. J. Cheon, E. Wi, M. Woo, T. T. Vu and M. Chang, Enhanced nitric oxide sensing performance of conjugated polymer films through incorporation of graphitic carbon nitride, *Int. J. Mol. Sci.*, 2023, **24**, 1158.
17 M. A. Ahmed, S. A. Mahmoud and A. A. Mohamed, Unveiling the photocatalytic potential of graphitic carbon nitride (gC_3N_4): a state-of-the-art review, *RSC Adv.*, 2024, **14**, 25629.
18 L. Wang and J. Yu, *Interface science and technology*, Elsevier, 2023, vol. 35, pp. 1–52.
19 J. Kim, K. Lee, S. Choi, N. Jo and Y. S. Nam, Catechol Quinone as an Electron-Shuttling Spot Conjugated to Graphitic Carbon Nitride for Enhancing Photocatalytic Reduction, *Chem. Mater.*, 2024, **36**, 5037.
20 M. Aresta, A. Dibenedetto and A. Angelini, Catalysis for the valorization of exhaust carbon: from CO_2 to chemicals, materials, and fuels. Technological use of CO_2, *Chem. Rev.*, 2014, **114**, 1709.
21 M. Z. Rahman and C. B. Mullins, Understanding charge transport in carbon nitride for enhanced photocatalytic solar fuel production, *Acc. Chem. Res.*, 2018, **52**, 248.
22 D. Qin, *et al.*, Recent advances in two-dimensional nanomaterials for photocatalytic reduction of CO_2: insights into performance, theories and perspective, *J. Mater. Chem. A*, 2020, **8**, 19156.
23 Z. Zhang, Progress and perspectives of electrochemical CO_2 reduction on copper in aqueous electrolyte, *Chem. Rev.*, 2019, **119**, 119.
24 V. Kumaravel, J. Bartlett and S. C. Pillai, Photoelectrochemical Conversion of Carbon Dioxide (CO_2) into Fuels and Value-Added Products, *ACS Energy Lett.*, 2020, **5**, 486.
25 R. Gandhi, A. Moses and S. S. Baral, Fundamental study of the photocatalytic reduction of CO_2: a short review of thermodynamics, kinetics and mechanisms, *Chem. Process Eng.*, 2022, **43**, 223.
26 L. Liu, S. Wang, H. Huang, Y. Zhang and T. Ma, Surface sites engineering on semiconductors to boost photocatalytic CO_2 reduction, *Nano Energy*, 2020, **75**, 104959.
27 B. Petrovic, M. Gorbounov and S. M. Soltani, Influence of surface modification on selective CO_2 adsorption: a technical review on mechanisms and methods, *Microporous Mesoporous Mater.*, 2021, **312**, 110751.
28 X. Wang, F. Wang, Y. Sang and H. Liu, Full-spectrum solar-light-activated photocatalysts for light–chemical energy conversion, *Adv. Energy Mater.*, 2017, **7**, 1700473.
29 A. Nawaz, A. Kuila, N. S. Mishra, K. H. Leong, L. C. Sim, P. Saravanan and M. Jang, Challenges and implication of full solar spectrum-driven photocatalyst, *Rev. Chem. Eng.*, 2021, **37**, 533.
30 S. Peiris, H. B. de Silva, K. N. Ranasinghe, S. V. Bandara and I. R. Perera, Recent development and future prospects of TiO_2 photocatalysis, *J. Chin. Chem. Soc.*, 2021, **68**, 738.
31 C. Hiragond, N. Powar, J. Lee and S. I. In, Single-Atom Catalysts (SACs) for Photocatalytic CO_2 Reduction with H_2O: Activity, Product Selectivity, Stability, and Surface Chemistry, *Small*, 2022, **18**(29), 2201428.
32 G. Z. S. Ling, S. F. Ng and W. J. Ong, Tailor-engineered 2D cocatalysts: harnessing electron–hole redox center of 2D g-C_3N_4 photocatalysts toward solar-to-chemical conversion and environmental purification, *Adv. Funct. Mater.*, 2022, **32**, 2111875.
33 K. Huang, C. Li, H. Li, G. Ren, L. Wang, W. Wang and X. Meng, Photocatalytic applications of two-dimensional Ti_3C_2 MXenes: a review, *ACS Appl. Nano Mater.*, 2020, **3**, 9581.
34 J. Ma, T. J. Miao and J. Tang, Charge carrier dynamics and reaction intermediates in heterogeneous photocatalysis by time-resolved spectroscopies, *Chem. Soc. Rev.*, 2022, **51**, 5777.
35 S. Bhattacharyya, *Carbon Superstructures: From Quantum Transport to Quantum Computation*, CRC Press, 2024.
36 G. R. Bhimanapati, *et al.*, Recent advances in two-dimensional materials beyond graphene, *ACS Nano*, 2015, **9**, 11509.
37 T. Enoki, Y. Kobayashi and K.-I. Fukui, Electronic structures of graphene edges and nanographene, *Int. Rev. Phys. Chem.*, 2007, **26**, 609.
38 Z. Zhen and H. Zhu, Structure and Properties of Graphene, *Graphene*, 2018, 1–12.
39 R. Geetha Bai, K. Muthoosamy, S. Manickam and A. Hilal-Alnaqbi, Graphene-based 3D scaffolds in tissue engineering: fabrication, applications, and future scope in liver tissue engineering, *Int. J. Nanomed.*, 2019, **14**, 5753–5783.
40 A. Kaplan, Z. Yuan, J. D. Benck, A. G. Rajan, X. S. Chu, Q. H. Wang and M. S. Strano, Current and future directions in electron transfer chemistry of graphene, *Chem. Soc. Rev.*, 2017, **46**, 4530.
41 N. Zhang, M.-Q. Yang, S. Liu, Y. Sun and Y.-J. Xu, Waltzing with the versatile platform of graphene to synthesize composite photocatalysts, *Chem. Rev.*, 2015, **115**, 10307.

42 H. Grajek, J. Jonik, Z. Witkiewicz, T. Wawer and M. Purchała, Applications of graphene and its derivatives in chemical analysis, *Crit. Rev. Anal. Chem.*, 2020, **50**, 445.
43 C. Li, C. Zheng, F. Cao, Y. Zhang and X. Xia, The development trend of graphene derivatives, *J. Electron. Mater.*, 2022, **51**, 4107.
44 J. Narayan and K. Bezborah, Recent advances in the functionalization, substitutional doping and applications of graphene/graphene composite nanomaterials, *RSC Adv.*, 2024, **14**, 13413.
45 R. Ghosh, M. Aslam and H. Kalita, Graphene derivatives for chemiresistive gas sensors: a review, *Mater. Today Commun.*, 2022, **30**, 103182.
46 R. Singh, *et al.*, Synthesis of Three-Dimensional Reduced-Graphene Oxide from Graphene Oxide, *J. Nanomater.*, 2022, **2022**, 8731429.
47 A. Ahmed, A. Singh, S.-J. Young, V. Gupta, M. Singh and S. Arya, Synthesis techniques and advances in sensing applications of reduced graphene oxide (rGO) Composites: a review, *Composites, Part A*, 2023, **165**, 107373.
48 A. Mondal, A. Prabhakaran, S. Gupta and V. R. Subramanian, Boosting photocatalytic activity using reduced graphene oxide (RGO)/semiconductor nanocomposites: issues and future scope, *ACS Omega*, 2021, **6**, 8734.
49 P. Jadhav and G. M. Joshi, Recent trends in Nitrogen doped polymer composites: a review, *J. Polym. Res.*, 2021, **28**, 73.
50 N. Sohal, B. Maity and S. Basu, Recent advances in heteroatom-doped graphene quantum dots for sensing applications, *RSC Adv.*, 2021, **11**, 25586.
51 M. B. Arvas, H. Gürsu, M. Gencten and Y. Sahin, Preparation of different heteroatom doped graphene oxide based electrodes by electrochemical method and their supercapacitor applications, *J. Energy Storage*, 2021, **35**, 102328.
52 S. J. Lee, *et al.*, Heteroatom-doped graphene-based materials for sustainable energy applications: a review, *Renewable Sustainable Energy Rev.*, 2021, **143**, 110849.
53 F. Zhang, E. Alhajji, Y. Lei, N. Kurra and H. N. Alshareef, Highly doped 3D graphene Na-ion battery anode by laser scribing polyimide films in nitrogen ambient, *Adv. Energy Mater.*, 2018, **8**, 1800353.
54 E. Umar, M. Ikram, J. Haider, W. Nabgan, M. Imran and G. Nazir, 3D graphene-based material: overview, perspective, advancement, energy storage, biomedical engineering and environmental applications a bibliometric analysis, *J. Environ. Chem. Eng.*, 2023, **11**, 110339.
55 F. M. Vivaldi, *et al.*, Three-dimensional (3D) laser-induced graphene: structure, properties, and application to chemical sensing, *ACS Appl. Mater. Interfaces*, 2021, **13**, 30245.
56 W. Xiao, B. Li, J. Yan, L. Wang, X. Huang and J. Gao, Three dimensional graphene composites: preparation, morphology and their multi-functional applications, *Composites, Part A*, 2023, **165**, 107335.
57 A. M. Díez-Pascual, *Int. J. Mol. Sci.*, 2021, **22**, 7726.
58 A. Gutiérrez-Cruz, A. R. Ruiz-Hernández, J. F. Vega-Clemente, D. G. Luna-Gazcón and J. Campos-Delgado, A review of top-down and bottom-up synthesis methods for the production of graphene, graphene oxide and reduced graphene oxide, *J. Mater. Sci.*, 2022, **57**, 14543.
59 A. Gutiérrez-Cruz, A. R. Ruiz-Hernández, J. F. Vega-Clemente, D. G. Luna-Gazcón and J. Campos-Delgado, A review of top-down and bottom-up synthesis methods for the production of graphene, graphene oxide and reduced graphene oxide, *J. Mater. Sci.*, 2022, **57**, 14543.
60 E. Boateng, A. R. Thiruppathi, C.-K. Hung, D. Chow, D. Sridhar and A. Chen, Functionalization of graphene-based nanomaterials for energy and hydrogen storage, *Electrochim. Acta*, 2023, **452**, 142340.
61 D. S. Rakshe, P. William, M. Jawale, A. Pawar, S. K. Korde and N. Deshpande, Synthesis and characterization of graphene based nanomaterials for energy applications, *J. Nano- Electron. Phys.*, 2023, **15**, 3020.
62 J. M. Tour, Top-down versus bottom-up fabrication of graphene-based electronics, *Chem. Mater.*, 2014, **26**, 163.
63 A. L. Olatomiwa, T. Adam, S. C. Gopinath, S. Y. Kolawole, O. H. Olayinka and U. Hashim, Graphene synthesis, fabrication, characterization based on bottom-up and top-down approaches: an overview, *J. Semiconductors*, 2022, **43**, 61101.
64 R. Boddula, N. Borane, N. Odedara and J. Singh, *Graphene-Based Nanomaterials*, CRC Press, 2024, pp. 33–46.
65 H. Jiang, Chemical preparation of graphene-based nanomaterials and their applications in chemical and biological sensors, *Small*, 2011, **7**, 2413.
66 N. Borane, S. Aralekallu, R. Boddula, J. Singh and M. D. Kurkuri, *Carbon-Based Nanomaterials in Biosystems*, Elsevier, 2024, pp. 91–120.
67 B. C. Brodie, On the atomic weight of graphite, *Philos. Trans. R. Soc. London*, 1859, **149**, 249.
68 D. C. Marcano, *et al.*, Improved synthesis of graphene oxide, *ACS Nano*, 2010, **4**, 4806.
69 H. L. Poh, F. Šaněk, A. Ambrosi, G. Zhao, Z. Sofer and M. Pumera, Graphenes prepared by Staudenmaier, Hofmann and Hummers' methods with consequent thermal exfoliation exhibit very different electrochemical properties, *Nanoscale*, 2012, **4**, 3515.
70 L. Shahriary and A. A. Athawale, Graphene oxide synthesized by using modified hummers approach, *Int. J. Renew. Energy Environ. Eng.*, 2014, **2**, 58.
71 T. Dzhabiev, N. Denisov, D. Moiseev and A. Shilov, Formation of ozone during the reduction of potassium permanganate in sulfuric acid solutions, *Russ. J. Phys. Chem. A*, 2005, **79**, 1755.
72 W. Gao, *et al.*, Ozonated graphene oxide film as a proton-exchange membrane, *Angew. Chem., Int. Ed.*, 2014, **53**, 3588.
73 M. Muradov, E. Huseynov, M. Conradi, M. Malok, T. Sever and M. B. Baghirov, Effects of gamma radiation on the properties of GO/PVA/AgNW nanocomposites, *RSC Adv.*, 2025, **15**, 13574.
74 S. K. Sharma and S. Sharma, Synthesis of Graphene Oxide and Impact of Its Functionalization in the Wastewater Treatment, *Chem. Eng. Technol.*, 2025, **48**, 70009.

75 C. Han, M.-Q. Yang, N. Zhang and Y.-J. Xu, Enhancing the visible light photocatalytic performance of ternary CdS–(graphene–Pd) nanocomposites via a facile interfacial mediator and co-catalyst strategy, *J. Mater. Chem. A*, 2014, **2**, 19156.
76 Y. Li, Z. Zhang, L. Pei, X. Li, T. Fan, J. Ji, J. Shen and M. Ye, Multifunctional photocatalytic performances of recyclable Pd–$NiFe_2O_4$/reduced graphene oxide nanocomposites via different co-catalyst strategy, *Appl. Catal., B*, 2016, **190**, 1.
77 D. Maarisetty and S. S. Baral, Synergistic effect of dual electron-cocatalyst modified photocatalyst and methodical strategy for better charge separation, *Appl. Surf. Sci.*, 2019, **489**, 930.
78 R. Akhter, S. Hussain and S. S. Maktedar, Advanced graphene-based (photo & electro) catalysts for sustainable & clean energy technologies, *New J. Chem.*, 2024, **48**, 437.
79 L. Ye, J. Fu, Z. Xu, R. Yuan and Z. Li, Facile one-pot solvothermal method to synthesize sheet-on-sheet reduced graphene oxide (RGO)/$ZnIn_2S_4$ nanocomposites with superior photocatalytic performance, *ACS Appl. Mater. Interfaces*, 2014, **6**, 3483.
80 N. Meng, Y. Zhou, W. Nie and P. Chen, Synthesis of CdS-decorated RGO nanocomposites by reflux condensation method and its improved photocatalytic activity, *J. Nanopart. Res.*, 2016, **18**, 241.
81 J. Prakash, Mechanistic insights into graphene oxide driven photocatalysis as Co-catalyst and sole catalyst in degradation of organic dye pollutants, *Photochem*, 2022, **2**, 651.
82 F. Khan, M. S. Khan, S. Kamal, M. Arshad, S. I. Ahmad and S. A. Nami, Recent advances in graphene oxide and reduced graphene oxide based nanocomposites for the photodegradation of dyes, *J. Mater. Chem. C*, 2020, **8**, 15940.
83 A. Mondal and A. Vomiero, 2D transition metal dichalcogenides-based electrocatalysts for hydrogen evolution reaction, *Adv. Funct. Mater.*, 2022, **32**, 2208994.
84 N. H. Shudin, M. Aziz, M. H. D. Othman, M. Tanemura and M. Z. M. Yusop, The role of solid, liquid and gaseous hydrocarbon precursors on chemical vapor deposition grown carbon nanomaterials' growth temperature, *Synth. Met.*, 2021, **274**, 116735.
85 P. Chavalekvirat, W. Hirunpinyopas, K. Deshsorn, K. Jitapunkul and P. Iamprasertkun, Liquid phase exfoliation of 2D materials and its electrochemical applications in the data-driven future, *Precis. Chem.*, 2024, **2**, 300.
86 T. Huang, F. Bing, L. Peipei, Z. Zhang, N. Qi, M. Zonghu, L. Kai and L. Qiang, Hydrothermal N-doping assisted synthesis of poplar sawdust-derived porous carbons for carbon capture, *J. Fuel Chem. Technol.*, 2025, **53**, 1191.
87 N. Zhang, Y. Zhang and Y.-J. Xu, Recent progress on graphene-based photocatalysts: current status and future perspectives, *Nanoscale*, 2012, **4**, 5792.
88 X. An and C. Y. Jimmy, Graphene-based photocatalytic composites, *RSC Adv.*, 2011, **1**, 1426.
89 F. Saeedi, R. Ansari and M. Haghgoo, Recent Advances of Graphene-Based Wearable Sensors: Synthesis, Fabrication, Performance, and Application in Smart Device, *Adv. Mater. Interfaces*, 2025, **12**, 2500093.
90 B. C. Yallur, *et al.*, Recent Advances in Graphene-Based Metal Oxide Composites for Supercapacitors: A Comprehensive Review, *Adv. Sustainable Syst.*, 2025, **9**, 2500121.
91 H. S. Biswas, A. K. Kundu and S. S. Biswas, *Recent Advancement of Graphene-TiO_2 Composite Nanomaterials and Their Applications in Energy Storage and Conversion: Novel Functions and Future Prospects Explored*, 2025, p. 425, DOI: 10.4018/979-8-3693-9316-1.ch014.
92 Y. Zhang, H. Wang and J. Zhang, Application of Graphene-Based Solar Driven Interfacial Evaporation-Coupled Photocatalysis in Water Treatment, *Catalysts*, 2025, **15**, 336.
93 T. Shahzad, S. Nawaz, H. Jamal, T. Shahzad, F. Akhtar and U. Kamran, A Review on Cutting-Edge Three-Dimensional Graphene-Based Composite Materials: Redefining Wastewater Remediation for a Cleaner and Sustainable World, *J. Compos. Sci.*, 2025, **9**, 18.
94 A. Badoni, *et al.*, Recent progress in understanding the role of graphene oxide, TiO_2 and graphene oxide-TiO_2 nanocomposites as multidisciplinary photocatalysts in energy and environmental applications, *Catal. Sci. Technol.*, 2025, **15**, 1702.
95 Y. Wu, C. Wang, L. Wang and C. Hou, Recent Advances in Iron Oxide-Based Heterojunction Photo-Fenton Catalysts for the Elimination of Organic Pollutants, *Catalysts*, 2025, **15**, 391.
96 A. K. Potbhare, *et al.*, Bioinspired graphene-based metal oxide nanocomposites for photocatalytic and electrochemical performances: an updated review, *Nanoscale Adv.*, 2024, **6**, 2539.
97 T. Xu, J. Wang, X. Yu, Y. Niu, H. Li, Y. Wu, M. Li and J. Rong, A new generation of functional desalted carbon and nitrogen membrane with photocatalytic and adsorption properties, *Comput. Mater. Sci.*, 2025, **258**, 114014.
98 A. Khalajiolyaie and C. Jian, Advances in Graphene-Based Materials for Metal Ion Sensing and Wastewater Treatment: A Review, *Environments*, 2025, **12**, 43.
99 W. Gao, H. Chi, Y. Xiong, J. Ye, Z. Zou and Y. Zhou, Comprehensive insight into construction of active sites toward steering photocatalytic CO_2 conversion, *Adv. Funct. Mater.*, 2024, **34**, 2312056.
100 S. Wang, M. Xu, T. Peng, C. Zhang, T. Li, I. Hussain, J. Wang and B. Tan, Porous hypercrosslinked polymer-TiO_2-graphene composite photocatalysts for visible-light-driven CO_2 conversion, *Nat. Commun.*, 2019, **10**, 676.
101 F.-X. Liang, Y. Gao, C. Xie, X.-W. Tong, Z.-J. Li and L.-B. Luo, Recent advances in the fabrication of graphene–ZnO heterojunctions for optoelectronic device applications, *J. Mater. Chem. C*, 2018, **6**, 3815.
102 S. Chandrasekaran, J. S. Chung, E. J. Kim and S. H. Hur, Exploring complex structural evolution of graphene oxide/ZnO triangles and its impact on photoelectrochemical water splitting, *Chem. Eng. J.*, 2016, **290**, 465.
103 X. Li, J. Yu, M. Jaroniec and X. Chen, Cocatalysts for selective photoreduction of CO_2 into solar fuels, *Chem. Rev.*, 2019, **119**, 3962.

104 P. M. Gawal, J. Ishrat, K. Bhattacharyya and A. K. Golder, Experimental and Theoretical Studies on Photocatalytic CO_2 Reduction to HCOOH by Biomass-Derived Carbon Dots Embedded Phytochemical-Based CdS Quantum Dots, *Langmuir*, 2025, **41**, 11161.

105 H. V. Babu, M. M. Bai and M. Rajeswara Rao, Functional π-conjugated two-dimensional covalent organic frameworks, *ACS Appl. Mater. Interfaces*, 2019, **11**, 11029.

106 L. Jing, P. Li, Z. Li, D. Ma and J. Hu, Influence of π–π interactions on organic photocatalytic materials and their performance, *Chem. Soc. Rev.*, 2025, **54**, 2054.

107 Y. Li, L. Wang, X. Gao, Y. Xue, B. Li and X. Zhu, Construction of a graphitic carbon nitride-based photocatalyst with a strong built-in electric field via π–π stacking interactions boosting photocatalytic CO_2 reduction, *J. Mater. Chem. A*, 2024, **12**, 7807.

108 K. Jayaramulu, *et al.*, Graphene-based metal–organic framework hybrids for applications in catalysis, environmental, and energy technologies, *Chem. Rev.*, 2022, **122**, 17241.

109 J. Yang, Z. Chen, L. Zhang and Q. Zhang, Covalent organic frameworks for photocatalytic reduction of carbon dioxide: a review, *ACS Nano*, 2024, **18**, 21804.

110 I. Ahmad, *et al.*, Recent progress in ZnO-based heterostructured photocatalysts: a review, *Mater. Sci. Semicond. Process.*, 2024, **180**, 108578.

111 I. Ahmad, S. Shukrullah, M. Y. Naz and H. N. Bhatti, Dual S-scheme ZnO–g-C_3N_4–CuO heterosystem: a potential photocatalyst for H_2 evolution and wastewater treatment, *React. Chem. Eng.*, 2023, **8**, 1159.

112 I. Ahmad, S. Shukrullah, M. Y. Naz, H. N. Bhatti and A. Cu, medium designed Z-scheme ZnO–Cu–CdS heterojunction photocatalyst for stable and excellent H_2 evolution, methylene blue degradation, and CO_2 reduction, *Dalton Trans.*, 2023, **52**, 6343.

113 I. Ahmad, S. A. AlFaify, K. M. Alanezi, M. Q. Alfaifi, M. M. Abduljawad and Y. Liu, Improved hydrogen production performance of an S-scheme Nb_2O_5/La_2O_3 photocatalyst, *Dalton Trans.*, 2025, **54**, 1402.

114 I. Ahmad, *et al.*, Boosted hydrogen evolution activity from Sr doped ZnO/CNTs nanocomposite as visible light driven photocatalyst, *Int. J. Hydrogen Energy*, 2021, **46**, 26711.

115 I. Ahmad, M. Q. Alfaifi, S. Ben Ahmed, M. M. Abduljawad, Y. A. Alassmy, S. A. Alshuhri and T. L. Tamang, Strategies for optimizing sunlight conversion in semiconductor photocatalysts: a review of experimental and theoretical insights, *Int. J. Hydrogen Energy*, 2024, **96**, 1006.

116 M. T. Vu, D. Thatikayala and B. Min, Porous reduced-graphene oxide supported hollow titania (rGO/TiO_2) as an effective catalyst for upgrading electromethanogenesis, *Int. J. Hydrogen Energy*, 2022, **47**, 1121.

117 J. Wu and M. Gong, ZnO/graphene heterostructure nanohybrids for optoelectronics and sensors, *J. Appl. Phys.*, 2021, **130**, 70905.

118 Z. Tan, R. Wang, S. Yang, Z. Shi and D. Wang, Fabrication of Cu–Cu_2ON doped carbon with high photo-Fenton catalytic activity using a Cu–nicotinic acid framework: insight into structural transformation, *J. Mol. Struct.*, 2025, **1337**, 142248.

119 R. Chaturvedi, R. Pandey, S. Singhania and A. Garg, Synergic Energy Storage Performance of MoS_2/g-C_3N_4 composite on Screen-printed Carbon Electrode, *Electrochim. Acta*, 2025, **539**, 147090.

120 G. Bharath, *et al.*, Synthesis of TiO_2/RGO with plasmonic Ag nanoparticles for highly efficient photoelectrocatalytic reduction of CO_2 to methanol toward the removal of an organic pollutant from the atmosphere, *Environ. Pollut.*, 2021, **281**, 116990.

121 J. Wekalao, High-sensitivity graphene-MoS_2 hybrid metasurface biosensor with machine learning optimization for hemoglobin detection, *Plasmonics*, 2025.

122 D. Kanakaraju, D. N. Joseph, P. P. Natashya and A. Pace, Pioneering TiO_2/G-C_3N_4 Heterostructures for Enhanced Organic Pollutant Removal, *ChemistrySelect*, 2025, **10**, 202405101.

123 S. K. Behura, C. Wang, Y. Wen and V. Berry, Graphene–semiconductor heterojunction sheds light on emerging photovoltaics, *Nat. Photonics*, 2019, **13**, 312.

124 A. Di Bartolomeo, Graphene Schottky diodes: an experimental review of the rectifying graphene/semiconductor heterojunction, *Phys. Rep.*, 2016, **606**, 1.

125 Z. Zhu, I. Murtaza, H. Meng and W. Huang, Thin film transistors based on two dimensional graphene and graphene/semiconductor heterojunctions, *RSC Adv.*, 2017, **7**, 17387.

126 S. Behura, C. Wang, Y. Wen and V. Berry, Graphene–Semiconductor Heterojunction Sheds Light on Emerging Photovoltaics, *Nat. Photonics*, 2019, **13**, 312.

127 Y.-J. Kim, J.-H. Lee and G.-C. Yi, Vertically aligned ZnO nanostructures grown on graphene layers, *Appl. Phys. Lett.*, 2009, **95**, 213101.

128 D. Maeso, A. Castellanos-Gomez, N. Agraït and G. Rubio-Bollinger, Fast Yet Quantum-Efficient Few-Layer Vertical MoS_2 Photodetectors, *Adv. Electron. Mater.*, 2019, **5**, 1900141.

129 X. Ge, W. Qin, H. Zhang, G. Wang, Y. Zhang and C. Yu, A three-dimensional porous Co@C/carbon foam hybrid monolith for exceptional oil–water separation, *Nanoscale*, 2019, **11**, 12161.

130 X. Xu, X. Zhang, C. Hu, Y. Zheng, B. Lei, Y. Liu and J. Zhuang, Construction of $NaYF_4$:Yb,Er(Tm)@CDs composites for enhancing red and NIR upconversion emission, *J. Mater. Chem. C*, 2019, **7**, 6231.

131 A. Singh, S. Chahal, H. Dahiya, A. Goswami and S. Nain, Synthesis of Ag nanoparticle supported graphene/multi-walled carbon nanotube based nanohybrids for photodegradation of toxic dyes, *Mater. Express*, 2021, **11**, 936.

132 A. Singh, S. Chahal, H. Dahiya, A. Goswami and S. Nain, Synthesis of Ag nanoparticle supported graphene/multi-walled carbon nanotube based nanohybrids for photodegradation of toxic dyes, *Materials Express*, 2021, **11**, 936.

133 Q. Ding, B. Song, P. Xu and S. Jin, Efficient electrocatalytic and photoelectrochemical hydrogen generation using MoS_2 and related compounds, *Chem*, 2016, **1**, 699.

134 D. Vikraman, K. Akbar, S. Hussain, G. Yoo, J.-Y. Jang, S.-H. Chun, J. Jung and H. J. Park, Direct synthesis of thickness-tunable MoS_2 quantum dot thin layers: optical, structural and electrical properties and their application to hydrogen evolution, *Nano Energy*, 2017, **35**, 101.

135 S. Chen and Y. Pan, Enhancing catalytic properties of noble metal@ MoS_2/WS_2 heterojunction for the hydrogen evolution reaction, *Appl. Surf. Sci.*, 2022, **591**, 153168.

136 D. Zheng, G. Zhang, Y. Hou and X. Wang, Layering MoS_2 on soft hollow g-C_3N_4 nanostructures for photocatalytic hydrogen evolution, *Appl. Catal., A*, 2016, **521**, 2.

137 Z. Wang, J. Huang, J. Mao, Q. Guo, Z. Chen and Y. Lai, Metal–organic frameworks and their derivatives with graphene composites: preparation and applications in electrocatalysis and photocatalysis, *J. Mater. Chem. A*, 2020, **8**, 2934.

138 E. F. Joel and G. Lujanienė, Progress in graphene oxide hybrids for environmental applications, *Environments*, 2022, **9**, 153.

139 Y.-J. Park, H. Lee, H. L. Choi, M. C. Tapia, C. Y. Chuah and T.-H. Bae, Mixed-dimensional nanocomposites based on 2D materials for hydrogen storage and CO_2 capture, *npj 2D Mater. Appl.*, 2023, **7**, 61.

140 T. Zhou, *et al.*, Polyethyleneimine-induced in-situ chemical epitaxial growth ultrathin 2D/2D graphene carbon nitride intralayer heterojunction with elevating photocatalytic activity: performances and mechanism insight, *Int. J. Hydrogen Energy*, 2024, **51**, 884.

141 T. A. Shifa, F. Wang, Y. Liu and J. He, Heterostructures Based on 2D Materials: A Versatile Platform for Efficient Catalysis, *Adv. Mater.*, 2018, **31**, 1804828.

142 H. Boumeriame, *et al.*, Graphitic carbon nitride/few-layer graphene heterostructures for enhanced visible-LED photocatalytic hydrogen generation, *Int. J. Hydrogen Energy*, 2022, **47**, 25555.

143 H. Li, B. Zhu, B. Cheng, G. Luo, J. Xu and S. Cao, Single-atom Cu anchored on N-doped graphene/carbon nitride heterojunction for enhanced photocatalytic H_2O_2 production, *J. Mater. Sci. Technol.*, 2023, **161**, 192.

144 M. Chen, M. Li, S. L. J. Lee, X. Zhao and S. Lin, Constructing novel graphitic carbon nitride-based nanocomposites-from the perspective of material dimensions and interfacial characteristics, *Chemosphere*, 2022, **302**, 134889.

145 D. Adekoya, S. Zhang and M. Hankel, 1D/2D C_3N_4/graphene composite as a preferred anode material for lithium ion batteries: importance of heterostructure design via DFT computation, *ACS Appl. Mater. Interfaces*, 2020, **12**, 25875.

146 K. Sridharan, S. Shenoy, S. G. Kumar, C. Terashima, A. Fujishima and S. Pitchaimuthu, Advanced two-dimensional heterojunction photocatalysts of stoichiometric and non-stoichiometric bismuth oxyhalides with graphitic carbon nitride for sustainable energy and environmental applications, *Catalysts*, 2021, **11**, 426.

147 X. Li, *et al.*, 2D-1D-2D multi-interfacial-electron transfer scheme enhanced g-C_3N_4/MWNTs/rGO hybrid composite for accelerating CO_2 photoreduction, *J. Alloys Compd.*, 2023, **940**, 168796.

148 J. Jia, Q. Zhang, K. Li, Y. Zhang, E. Liu and X. Li, Recent advances on g-C_3N_4-based Z-scheme photocatalysts: structural design and photocatalytic applications, *Int. J. Hydrogen Energy*, 2023, **48**, 196.

149 X. Zeng, Z. Wang, G. Wang, T. R. Gengenbach, D. T. McCarthy, A. Deletic, J. Yu and X. Zhang, Highly dispersed TiO_2 nanocrystals and WO_3 nanorods on reduced graphene oxide: Z-scheme photocatalysis system for accelerated photocatalytic water disinfection, *Appl. Catal., B*, 2017, **218**, 163.

150 J. Low, C. Jiang, B. Cheng, S. Wageh, A. A. Al-Ghamdi and J. Yu, A review of direct Z-scheme photocatalysts, *Small methods*, 2017, **1**, 1700080.

151 X. Miao, X. Shen, J. Wu, Z. Ji, J. Wang, L. Kong, M. Liu and C. Song, Fabrication of an all solid Z-scheme photocatalyst g-C_3N_4/GO/AgBr with enhanced visible light photocatalytic activity, *Appl. Catal., A*, 2017, **539**, 104.

152 Z. Qian, B. Pathak, J. Nisar and R. Ahuja, Oxygen-and nitrogen-chemisorbed carbon nanostructures for Z-scheme photocatalysis applications, *J. Nanopart. Res.*, 2012, **14**, 895.

153 D. Zhou, D. Li and Z. Chen, Recent advances in ternary Z-scheme photocatalysis on graphitic carbon nitride based photocatalysts, *Front. Chem.*, 2024, **12**, 1359895.

154 M. Li, *et al.*, Novel Z-scheme visible-light photocatalyst based on $CoFe_2O_4$/BiOBr/Graphene composites for organic dye degradation and Cr(VI) reduction, *Appl. Surf. Sci.*, 2019, **478**, 744.

155 W. Li, X. Wang, M. Li, S.-A. He, Q. Ma and X. Wang, Construction of Z-scheme and pn heterostructure: three-dimensional porous g-C_3N_4/graphene oxide-Ag/AgBr composite for high-efficient hydrogen evolution, *Appl. Catal., B*, 2020, **268**, 118384.

156 Z. Chen, S. Sun and J. Prakash, Design and engineering of graphene nanostructures as independent solar-driven photocatalysts for emerging applications in the field of energy and environment, *Mol. Syst. Des. Eng.*, 2022, **7**, 213.

157 S. Huang, M. Hu, L. He, S. Ren, X. Wu and S. Cui, Construction of manganese ferrite/zinc ferrite anchored graphene-based hierarchical aerogel photocatalysts following Z-scheme electron transfer for visible-light-driven carbon dioxide reduction, *J. Colloid Interface Sci.*, 2025, **694**, 137678.

158 A. O. Oluwole, T. L. Yusuf, S. M. Tichapondwa, M. O. Daramola and S. A. Iwarere, Fabrication of $BiVO_4/Ag_2CrO_4$ heterojunction composites modified with graphene oxide for enhanced photoelectrochemical and photocatalytic performance, *RSC Adv.*, 2024, **14**, 38044.

159 M. Chu, J. Bian, Z. Zhang, Z. Zhao and L. Jing, Graphene-Regulated Interfacial Z-Scheme Charge Transfer for CO_2 Photoreduction to CO with Nearly 100% Selectivity, *J. Phys. Chem. C*, 2025, **129**, 8868.

160 M. T. Baig, Z. Zahid, M. Tauqeer, C.-H. Park, J. P. Park, C.-H. Choi, T. Yoon and A. Mohammad, State-of-the-art

developments in metal/metal oxide and graphene-based nano-hybrid systems for photocatalytic degradation of tetracycline antibiotics, *J. Ind. Eng. Chem.*, 2025, **148**, 69.

161 A. Meera, M. Mahalakshmi and B. Neppolian, The strategy on selecting the oxidation photocatalyst $NiWO_4$ as a co-catalyst to enhance the performance of TiO_2/rGO for H_2 production under solar light, *Int. J. Hydrogen Energy*, 2025, **144**, 186.

162 P.-Q. Wang, Y. Bai, P.-Y. Luo and J.-Y. Liu, Graphene–WO_3 nanobelt composite: elevated conduction band toward photocatalytic reduction of CO_2 into hydrocarbon fuels, *Catal. Commun.*, 2013, **38**, 82.

163 Y. Xia, B. Cheng, J. Fan, J. Yu and G. Liu, Near-infrared absorbing 2D/3D $ZnIn_2S_4$/N-doped graphene photocatalyst for highly efficient CO_2 capture and photocatalytic reduction, *Sci. China Mater.*, 2020, **63**, 552.

164 W.-J. Ong, L.-L. Tan, S.-P. Chai and S.-T. Yong, Graphene oxide as a structure-directing agent for the two-dimensional interface engineering of sandwich-like graphene–g-C_3N_4 hybrid nanostructures with enhanced visible-light photoreduction of CO_2 to methane, *Chem. Commun.*, 2015, **51**, 858.

165 H.-C. Hsu, *et al.*, Graphene oxide as a promising photocatalyst for CO_2 to methanol conversion, *Nanoscale*, 2013, **5**, 262.

166 I. Shown, *et al.*, Highly Efficient Visible Light Photocatalytic Reduction of CO_2 to Hydrocarbon Fuels by Cu-Nanoparticle Decorated Graphene Oxide, *Nano Lett.*, 2014, **14**, 6097.

167 J. Cheng, M. Zhang, G. Wu, X. Wang, J. Zhou and K. Cen, Photoelectrocatalytic Reduction of CO_2 into Chemicals Using Pt-Modified Reduced Graphene Oxide Combined with Pt-Modified TiO_2 Nanotubes, *Environ. Sci. Technol.*, 2014, **48**, 7076.

168 L. M. Pastrana-Martínez, A. M. T. Silva, N. N. C. Fonseca, J. R. Vaz, J. L. Figueiredo and J. L. Faria, Photocatalytic Reduction of CO_2 with Water into Methanol and Ethanol Using Graphene Derivative–TiO_2 Composites: Effect of pH and Copper(I) Oxide, *Top. Catal.*, 2016, **59**, 1279.

169 L.-L. Tan, W.-J. Ong, S.-P. Chai and A. R. Mohamed, Noble metal modified reduced graphene oxide/TiO_2 ternary nanostructures for efficient visible-light-driven photoreduction of carbon dioxide into methane, *Appl. Catal., B*, 2015, **166**, 251.

170 Z. Xiong, Y. Luo, Y. Zhao, J. Zhang, C. Zheng and J. C. S. Wu, Synthesis, characterization and enhanced photocatalytic CO_2 reduction activity of graphene supported TiO_2 nanocrystals with coexposed {001} and {101} facets, *Phys. Chem. Chem. Phys.*, 2016, **18**, 13186.

171 R. Gusain, P. Kumar, O. P. Sharma, S. L. Jain and O. P. Khatri, Reduced graphene oxide–CuO nanocomposites for photocatalytic conversion of CO_2 into methanol under visible light irradiation, *Appl. Catal., B*, 2016, **181**, 352.

172 L.-L. Tan, W.-J. Ong, S.-P. Chai and A. R. Mohamed, Photocatalytic reduction of CO_2 with H_2O over graphene oxide-supported oxygen-rich TiO_2 hybrid photocatalyst under visible light irradiation: process and kinetic studies, *Chem. Eng. J.*, 2017, **308**, 248.

173 Q. Zhang, L. Huang, S. Kang, C. Yin, Z. Ma, L. Cui and Y. Wang, CuO/Cu_2O nanowire arrays grafted by reduced graphene oxide: synthesis, characterization, and application in photocatalytic reduction of CO_2, *RSC Adv.*, 2017, **7**, 43642.

174 S. Sorcar, J. Thompson, Y. Hwang, Y. H. Park, T. Majima, C. A. Grimes, J. R. Durrant and S.-I. In, High-rate solar-light photoconversion of CO_2 to fuel: controllable transformation from C1 to C2 products, *Energy Environ. Sci.*, 2018, **11**, 3183.

175 S. Kumar, R. K. Yadav, K. Ram, A. Aguiar, J. Koh and A. J. F. N. Sobral, Graphene oxide modified cobalt metallated porphyrin photocatalyst for conversion of formic acid from carbon dioxide, *J. CO2 Util.*, 2018, **27**, 107.

176 P. Devi and J. P. Singh, Visible light induced selective photocatalytic reduction of CO_2 to CH_4 on In_2O_3-rGO nanocomposites, *J. CO2 Util.*, 2021, **43**, 101376.

177 X. Wang, Q. Li, C. Zhou, Z. Cao and R. Zhang, ZnO rod/reduced graphene oxide sensitized by α-Fe_2O_3 nanoparticles for effective visible-light photoreduction of CO_2, *J. Colloid Interface Sci.*, 2019, **554**, 335.

178 H.-T. Lien, *et al.*, Solar to hydrocarbon production using metal-free water-soluble bulk heterojunction of conducting polymer nanoparticle and graphene oxide, *J. Chem. Phys.*, 2021, **154**, 164707.

179 T. Wu, C. Zhu, D. Han, Z. Kang and L. Niu, Highly selective conversion of CO_2 to C_2H_6 on graphene modified chlorophyll Cu through multi-electron process for artificial photosynthesis, *Nanoscale*, 2019, **11**, 22980.

180 K. M. Kamal, *et al.*, Synergistic enhancement of photocatalytic CO_2 reduction by plasmonic Au nanoparticles on TiO_2 decorated N-graphene heterostructure catalyst for high selectivity methane production, *Appl. Catal., B*, 2022, **307**, 121181.

181 H. R. Park, A. U. Pawar, U. Pal, T. Zhang and Y. S. Kang, Enhanced solar photoreduction of CO_2 to liquid fuel over rGO grafted NiO–CeO_2 heterostructure nanocomposite, *Nano Energy*, 2021, **79**, 105483.

182 W. Tu, *et al.*, Robust Hollow Spheres Consisting of Alternating Titania Nanosheets and Graphene Nanosheets with High Photocatalytic Activity for CO_2 Conversion into Renewable Fuels, *Adv. Funct. Mater.*, 2012, **22**, 1215.

183 N. Nandal, P. K. Prajapati, B. M. Abraham and S. L. Jain, CO_2 to ethanol: a selective photoelectrochemical conversion using a ternary composite consisting of graphene oxide/copper oxide and a copper-based metal-organic framework, *Electrochim. Acta*, 2022, **404**, 139612.

184 J. Yu, J. Jin, B. Cheng and M. Jaroniec, A noble metal-free reduced graphene oxide–CdS nanorod composite for the enhanced visible-light photocatalytic reduction of CO_2 to solar fuel, *J. Mater. Chem. A*, 2014, **2**, 3407.

185 Y. T. Liang, B. K. Vijayan, O. Lyandres, K. A. Gray and M. C. Hersam, Effect of Dimensionality on the Photocatalytic

Behavior of Carbon–Titania Nanosheet Composites: Charge Transfer at Nanomaterial Interfaces, *J. Phys. Chem. Lett.*, 2012, **3**, 1760.

186 W. Tu, Y. Zhou, Q. Liu, S. Yan, S. Bao, X. Wang, M. Xiao and Z. Zou, An In Situ Simultaneous Reduction-Hydrolysis Technique for Fabrication of TiO_2-Graphene 2D Sandwich-Like Hybrid Nanosheets: Graphene-Promoted Selectivity of Photocatalytic-Driven Hydrogenation and Coupling of CO_2 into Methane and Ethane, *Adv. Funct. Mater.*, 2013, **23**, 1743.

187 S. Liu, B. Weng, Z.-R. Tang and Y.-J. Xu, Constructing one-dimensional silver nanowire-doped reduced graphene oxide integrated with CdS nanowire network hybrid structures toward artificial photosynthesis, *Nanoscale*, 2015, **7**, 861.

188 J. Hou, H. Cheng, O. Takeda and H. Zhu, Three-Dimensional Bimetal-Graphene-Semiconductor Coaxial Nanowire Arrays to Harness Charge Flow for the Photochemical Reduction of Carbon Dioxide, *Angew. Chem., Int. Ed.*, 2015, **54**, 8480.

189 X. An, K. Li and J. Tang, Cu_2O/Reduced Graphene Oxide Composites for the Photocatalytic Conversion of CO_2, *ChemSusChem*, 2014, **7**, 1086.

190 X. Li, Q. Wang, Y. Zhao, W. Wu, J. Chen and H. Meng, Green synthesis and photo-catalytic performances for ZnO-reduced graphene oxide nanocomposites, *J. Colloid Interface Sci.*, 2013, **411**, 69.

191 P. Li, Y. Zhou, H. Li, Q. Xu, X. Meng, X. Wang, M. Xiao and Z. Zou, All-solid-state Z-scheme system arrays of $Fe_2V_4O_{13}$/RGO/CdS for visible light-driving photocatalytic CO_2 reduction into renewable hydrocarbon fuel, *Chem. Commun.*, 2015, **51**, 800.

192 J. Park, T. Jin, C. Liu, G. Li and M. Yan, Three-Dimensional Graphene–TiO_2 Nanocomposite Photocatalyst Synthesized by Covalent Attachment, *ACS Omega*, 2016, **1**, 351.

193 M. Song, *et al.*, Facile synthesis of MOF–808/RGO-based 3D macroscopic aerogel for enhanced photoreduction CO_2, *J. Colloid Interface Sci.*, 2024, **668**, 471.

194 J. Zhang, S. Shao, D. Zhou, Q. Xu and T. Wang, ZnO nanowire arrays decorated 3D N-doped reduced graphene oxide nanotube framework for enhanced photocatalytic CO_2 reduction performance, *J. CO2 Util.*, 2021, **50**, 101584.

195 Y. T. Liang, B. K. Vijayan, K. A. Gray and M. C. Hersam, Minimizing Graphene Defects Enhances Titania Nanocomposite-Based Photocatalytic Reduction of CO_2 for Improved Solar Fuel Production, *Nano Lett.*, 2011, **11**, 2865.

196 B. Kaur, *et al.*, Catalytic performance of Graphdiyne for CO_2 reduction and charge dynamics progress, *J. Environ. Chem. Eng.*, 2025, 116904.

197 F.-Y. Liu, H.-L. Chen, K.-Y. Hsiao, Y.-M. Dai, C.-C. Chen and I.-C. Chen, Unveiling photochemical CO_2 reduction processes on $PbBiO_2I$/GO surfaces: insights from in situ Raman spectroscopy, *Appl. Catal., B*, 2025, **364**, 124844.

198 Z. Zhang, L. Li, S. Gao and P. Yang, Graphene interface modification to improve efficiency and stability at $MAPbI_3$/ZnO interface for perovskite solar cells: a first-principles study, *Sol. Energy*, 2025, **287**, 113236.

199 U. U. Rehman, R. S. Almufarij, A. Abd-Elwahed, K. U. Sahar, E. Hussain, A. Ashfaq, K. Mahmood and C.-M. Wang, Improving efficiency of germanium-based perovskite solar cells with graphene interface layer: a strategy to minimize charge recombination, *J. Phys. Chem. Solids*, 2025, **198**, 112487.

200 S. Fu, H. Zhang, K.-J. Tielrooij, M. Bonn and H. I. Wang, Tracking and controlling ultrafast charge and energy flow in graphene-semiconductor heterostructures, *The Innovation*, 2025, **6**, 100764.

201 X. Zhou, *et al.*, Weakness-complementing Z-scheme black phosphorus/TiO_2 heterojunction with efficient charge separation and photocatalytic overall water splitting activity, *J. Colloid Interface Sci.*, 2025, **689**, 137240.

202 A. Kamboukos, N. Todorova and I. Yarovsky, Exploring 2D Graphene-Based Nanomaterials for Biomedical Applications: A Theoretical Modeling Perspective, *Small Sci.*, 2025, **5**, 2400505.

203 S. Samajdar, M. Biswas, D. Sarkar, J. Pramanik, J. Mukhopadhyay and S. Ghosh, Double heterojunction photocatalysts: strategic fabrication and mechanistic insights towards sustainable fuel production, *Chem. Commun.*, 2025, **61**, 6069.

204 X. Zhu, Y. Hu, G. Wu, W. Chen and N. Bao, Two-dimensional nanosheets-based soft electro-chemo-mechanical actuators: recent advances in design, construction, and applications, *ACS Nano*, 2021, **15**, 9273.

205 X. Lan, N. Luo, Z. Li, J. Peng and H.-M. Cheng, Status and prospect of two-dimensional materials in electrolytes for all-solid-state lithium batteries, *ACS Nano*, 2024, **18**, 9285.

206 Z. Zhou, W. Qi, Z. Li, L. Yang, Z. Lin and R. Guan, N-P Type Charge Compensatory Synergistic Effect for Schottky and Efficient Photoelectrocatalysis Applications: Doping Mechanism in (Nb/Re)@WS_2/Graphene Heterojunctions, *Chem. – Eur. J.*, 2025, **31**, e202403963.

207 F. Gomes, *et al.*, Advancing Dye-Sensitized Solar Cells: Synergistic Effects of Polyaniline, Graphene Oxide, and Carbon Nanotubes for Enhanced Efficiency and Sustainability Developments, *Recent Pat. Nanotechnol.*, 2025, DOI: 10.2174/0118722105366556250402051103.

208 D. Das, M. Das, S. Sil, P. Sahu and P. P. Ray, Effect of Higher Carrier Mobility of the Reduced Graphene Oxide–Zinc Telluride Nanocomposite on Efficient Charge Transfer Facility and the Photodecomposition of Rhodamine B, *ACS Omega*, 2022, **7**, 26483, DOI: 10.1021/acsomega.2c02472.

209 G. S. Natarajamani, V. P. Kannan and S. Madanagurusamy, Synergistic ramifications of a sustainable ultra-sensitive NH_3 sensor: thermally reduced graphene oxide/ZnO hybrid composite for sub-PPM detection, *J. Environ. Chem. Eng.*, 2025, **13**, 116079.

210 T. Sewela, R. Ocaya and T. Malevu, Recent insights into the transformative role of Graphene-based/TiO_2 electron transport layers for perovskite solar cells, *Energy Sci. Eng.*, 2025, **13**, 4.

211 F. Ullah, B. H. Guan, M. Zafar, N. E. Hira, H. Khan and M. S. M. Saheed, Synergistic enhancement in PEC hydrogen production using novel GQDs and CuO modified TiO_2 based heterostructure photocatalyst, *Mater. Chem. Phys.*, 2025, **340**, 130781.

212 D. Maarisetty, R. Mary, D.-R. Hang, P. Mohapatra and S. S. Baral, The role of material defects in the photocatalytic CO_2 reduction: interfacial properties, thermodynamics, kinetics and mechanism, *J. CO_2 Util.*, 2022, **64**, 102175.

213 C. A. Celaya, C. Delesma, P. Valadés-Pelayo, O. A. Jaramillo-Quintero, C. O. Castillo-Araiza, L. Ramos, P. Sebastian and J. Muñiz, Exploring the potential of graphene oxide as a functional material to produce hydrocarbons via photocatalysis: theory meets experiment, *Fuel*, 2020, **271**, 117616.

214 M. Y. Akram, T. Ashraf, M. S. Jagirani, A. Nazir, M. Saqib and M. Imran, Recent advances in graphene-based single-atom photocatalysts for CO_2 reduction and H_2 production, *Catalysts*, 2024, **14**, 343.

215 J. O. Olowoyo, M. Kumar, B. Singh, V. O. Oninla, J. O. Babalola, H. Valdés, A. V. Vorontsov and U. Kumar, Self-assembled reduced graphene oxide-TiO_2 nanocomposites: synthesis, DFTB+ calculations, and enhanced photocatalytic reduction of CO_2 to methanol, *Carbon*, 2019, **147**, 385.

216 Y. Cui, X. Huang, T. Wang, L. Jia, Q. Nie, Z. Tan and H. Yu, Graphene quantum dots/carbon nitride heterojunction with enhanced visible-light driven photocatalysis of nitric oxide: an experimental and DFT study, *Carbon*, 2022, **191**, 502.

217 A. Olatomiwa, T. Adam, C. Edet, A. Adewale, A. Chik, M. Mohammed, S. C. Gopinath and U. Hashim, Recent advances in density functional theory approach for optoelectronics properties of graphene, *Heliyon*, 2023, **9**, 14279.

218 M. Khenfouch, M. Baïtoul and M. Maaza, White photoluminescence from a grown ZnO nanorods/graphene hybrid nanostructure, *Opt. Mater.*, 2012, **34**, 1320.

219 B. Weng and Y.-J. Xu, What if the electrical conductivity of graphene is significantly deteriorated for the graphene–semiconductor composite-based photocatalysis?, *ACS Appl. Mater. Interfaces*, 2015, **7**, 27948.

220 Y. Xiang, L. Xin, J. Hu, C. Li, J. Qi, Y. Hou and X. Wei, Advances in the applications of graphene-based nanocomposites in clean energy materials, *Crystals*, 2021, **11**, 47.

221 G. Marineau-Plante, *et al.*, Effect of mesogenic side groups on the redox, photophysical, and solar cell properties of diketopyrrolopyrrole-trans-bis (diphosphine) diethynylplatinum(II) polymers, *ACS Appl. Polym. Mater.*, 2021, **3**, 1087.

222 A. K. Worku and D. W. Ayele, Recent advances of graphene-based materials for emerging technologies, *Results Chem.*, 2023, **5**, 100971.

223 A. G. Al-Gamal, A. M. Elseman and K. I. Kabel, Advances in Nitrogen-Functionalized Graphene for Enhanced Photovoltaic Applications, *Solar RRL*, 2025, **9**, 2500002.

224 E. Flórez, C. Jimenez-Orozco and N. Acelas, Unravelling the influence of surface functional groups and surface charge on heavy metal adsorption onto carbonaceous materials: an in-depth DFT study, *Mater. Today Commun.*, 2024, **39**, 108647.

225 M. Yang, B. Qin, C. Si, X. Sun and B. Li, Electrochemical reactions catalyzed by carbon dots from computational investigations: functional groups, dopants, and defects, *J. Mater. Chem. A*, 2024, **12**, 2520.

226 Y. Li, W. Niu, T. Chen, Y. Sun and M. Yu, Integrating vacancy engineering and energy-level adapted coupling of electrocatalyst for enhancement of carbon dioxide conversion, *Appl. Catal., B*, 2023, **321**, 122037.

227 S. Xu and E. A. Carter, CO_2 photoelectrochemical reduction catalyzed by a GaP(001) photoelectrode, *ACS Catal.*, 2021, **11**, 1233.

228 X. Xu, C. Liu, Z. Sun, T. Cao, Z. Zhang, E. Wang, Z. Liu and K. Liu, Interfacial engineering in graphene bandgap, *Chem. Soc. Rev.*, 2018, **47**, 3059.

229 S. Nakaharai, T. Iijima, S. Ogawa, S. Suzuki, S.-L. Li, K. Tsukagoshi, S. Sato and N. Yokoyama, Conduction tuning of graphene based on defect-induced localization, *ACS Nano*, 2013, **7**, 5694.

230 M. Kumar Kumawat, S. Kumar and T. Mohanty, Tailoring functional properties of graphene oxide by defect-assisted surface and interface modifications, *J. Mater. Res.*, 2022, **37**, 3394.

231 I. Shtepliuk, Defect-induced modulation of a 2D ZnO/graphene heterostructure: exploring structural and electronic transformations, *Appl. Sci.*, 2023, **13**, 7243.

232 K. P. Dhakal, *et al.*, Local strain induced band gap modulation and photoluminescence enhancement of multilayer transition metal dichalcogenides, *Chem. Mater.*, 2017, **29**, 5124.

233 D. Maarisetty and S. S. Baral, Defect engineering in photocatalysis: formation, chemistry, optoelectronics, and interface studies, *J. Mater. Chem. A*, 2020, **8**, 18560.

234 M. Shen, L. Zhang and J. Shi, Defect engineering of photocatalysts towards elevated CO_2 reduction performance, *ChemSusChem*, 2021, **14**, 2635.

235 B. Wang, G. Du, S. Tan, S. Guo, Z. Zhu, G.-F. Huang, W.-Q. Huang and R. Jiang, Constructing a Double Type-Ii G-C_3N_4/CDS/MoS_2 (Gcsm) Heterojunction with Dual-Enhanced Redox Capability for Efficient Photocatalytic Pollutant Degradation, *J. Phys. D: Appl. Phys.*, 2025, **58**, 315102.

236 S. Zhang, X. Zhang, W. Shi, H. Weiyan and X. Wang, The Study on the Construction of S-Scheme G-C_3N_4/MOF Heterojunctions Through Interface and Built-In Electric Field Modulation and Their Photocatalytic Degradation Performance of Tetracycline, *Chem. Phys. Lett.*, 2025, **876**, 142195.

237 Y. Wang, Y. Liu, H. Zhang, X. Duan, J. Ma, H. Sun, W. Tian and S. Wang, Carbonaceous materials in structural dimensions for advanced oxidation processes, *Chem. Soc. Rev.*, 2025, **54**, 2436.

238 Q. Tian, Q. Li, T. Zhang, W. Huang, C. Zhao, B. Hu and X. Xu, Molecular Orbital Level Micro-Electric Field in

Green Fenton-Like Chemistry for Water Treatment: From Mechanism Understanding to Scale-Up Applications, *Adv. Mater.*, 2025, e09280.

239 N. N. Rabin, H. Ohmagari, M. S. Islam, M. R. Karim and S. Hayami, A procession on photocatalyst for solar fuel production and waste treatment, *J. Inclusion Phenom. Macrocyclic Chem.*, 2019, **94**, 263.

240 M. D. Ali, A. Starczewska, T. K. Das and M. Jesionek, Exploration of Sp-Sp^2 Carbon Networks: Advances in Graphyne Research and Its Role in Next-Generation Technologies, *Int. J. Mol. Sci.*, 2025, **26**, 5140.

241 F. Liu, G. Wei and B. Hu, A review on n-type chemical doping of graphene films: preparation, characterization and applications, *Nanoscale*, 2025, **17**, 21291.

242 L. K. Putri, W.-J. Ong, W. S. Chang and S.-P. Chai, Heteroatom doped graphene in photocatalysis: a review, *Appl. Surf. Sci.*, 2015, **358**, 2.

243 J. Jianga, Y. Zhanga, W. Suna, J. Penga, W. Shib, Y. Quc and E. Liud, A review of updated red phosphorus-based photocatalysts, *Comp. Funct. Mat.*, 2025, **1**, 20250101.

244 W. Zhu, B. Zhang, Y. Yang, M. Zhao, Y. Fang, Y. Cui and J. Tian, Enhanced Electrocatalytic Performance of P-Doped MoS_2/rGO Composites for Hydrogen Evolution Reactions, *Molecules*, 2025, **30**, 1205.

245 S. Zhi, Q. Dai, H. Wang, D. Wu, L. Zhao, C. Hu and L. Dai, Heteroatom-Doped Carbon Materials for Multifunctional Noncatalytic Applications, *ACS Nano*, 2025, **19**, 29860.

246 H. Noorizadeh, R. H. Al Omari, A. Kumar, A. F. Al-Hussainy, S. Mohammed, A. Sinha and S. Ray, Indium Phosphide Quantum Dots as Green Nanosystems for Environmental Detoxification: Surface Engineering, Photocatalytic Mechanisms, and Comparative Material Insights, *Environ. Sci.: Adv.*, 2025, **4**, 1553.

247 Z. A. Sandhu, U. Farwa, M. Danish, M. A. Raza, A. Talib, H. Amjad, R. Riaz and A. G. Al-Sehemi, Sustainability and photocatalytic performance of MOFs: synthesis strategies and structural insights, *J. Cleaner Prod.*, 2024, **470**, 143263.

248 D. S. Constantino, M. M. Dias, A. M. Silva, J. L. Faria and C. G. Silva, Intensification strategies for improving the performance of photocatalytic processes: a review, *J. Cleaner Prod.*, 2022, **340**, 130800.

249 S. Sadana, N. Rajamohan, R. Manivasagan, N. Raut, S. Paramasivam, G. Gatto and A. Kumar, Graphene-based materials for photocatalytic and environmental sensing applications, *Results Eng.*, 2025, **27**, 105725.

250 I. Razzaq, *et al.*, Graphene-Based Polymer Composites for High-Performance Chemical Sensing and Detection: A Critical Review, *Adv. Mater. Technol.*, 2025, **10**, e00578.

251 R. Atchudan, T. N. J. I. Edison, S. Perumal, D. Karthikeyan and Y. R. Lee, Facile synthesis of zinc oxide nanoparticles decorated graphene oxide composite via simple solvothermal route and their photocatalytic activity on methylene blue degradation, *J. Photochem. Photobiol., B*, 2016, **162**, 500.

252 M. Ahmad, E. Ahmed, Z. Hong, N. Khalid, W. Ahmed and A. Elhissi, Graphene–Ag/ZnO nanocomposites as high performance photocatalysts under visible light irradiation, *J. Alloys Compd.*, 2013, **577**, 717.

253 X. Liu, A. Hu, Z. Liu, K. Ding, W. Xia, H. Shangguan, C. Zhang and T. Fu, Review on fundamental and recent advances of strain engineering for enhancing photocatalytic CO_2 reduction, *Adv. Energy Mater.*, 2025, **15**, 2405320.

254 L. T. Mambiri, Physicochemical Modulation of Polycaprolactone/Nanohydroxyapatite Properties *via* Graphene Oxide Nanoscroll Interfacial Bridging for Bone Tissue Engineering, University of Louisiana at Lafayette, 2025.

255 L. Jiang, X. Zhi, X. Bai and Y. Jiao, Atomic-level insights into cation-mediated mechanism in electrochemical nitrogen reduction, *J. Am. Chem. Soc.*, 2025, **147**, 16935.

256 G. G. Nezhad, H. Esfandian and M. S. Lashkenari, Synthesis and Electrocatalytic Performance of Cu–Pb/RGO Composite for Efficient CO_2 Reduction to Methanol, *Results Eng.*, 2025, **26**, 105436.

257 S. J. Armaković, S. Armaković, A. Bilić and M. M. Savanović, ZnO-Based Photocatalysts: Synergistic Effects of Material Modifications and Machine Learning Optimization, *Catalysts*, 2025, **15**, 793.

258 Q. Adfar, S. Hussain and S. S. Maktedar, Insights into energy and environmental sustainability through photoactive graphene-based advanced materials: perspectives and promises, *New J. Chem.*, 2025, **49**, 2511.

259 S. Sambyal, P. Raizada, A. Chawla, A. A. P. Khan, S. Thakur, V.-H. Nguyen and P. Singh, Tuning ZnCdS heterostructures for enhanced photocatalysis: hybrid architectures for sustainable energy and environmental applications, *J. Mater. Chem. A*, 2025, **13**, 29833.

260 G. I. Edo, *et al.*, Green Biosynthesis of Nanoparticles Using Plant Extracts: Mechanisms, Advances, Challenges, and Applications, *Bionanoscience*, 2025, **15**, 267.

261 A. Kumar, S. R. Shah, T. J. Jayeoye, A. Kumar, A. Parihar, B. Prajapati6, S. Singh and D. U. Kapoor, *Front. Nanotechnol.*, 2023, **5**, 1175149.

262 G. B. Mahendran, S. J. Ramalingam, J. B. B. Rayappan, S. Kesavan, T. Periathambi and N. Nesakumar, Green preparation of reduced graphene oxide by Bougainvillea glabra flower extract and sensing application, *J. Mater. Sci.: Mater. Electron.*, 2020, **31**, 14345.

263 J. Singh, D. D. Nguyen, P. Leclere and P. Nguyen-Tri, Recent Advancements in Graphene-Based Nanocomposites for Enhanced Photocatalysis in Environmental Remediation: A Comprehensive Review, *Rev. Environ. Contam. Toxicol.*, 2025, **263**, 13.

264 P. Rana, P. Singh, V. Puri, Q. Van Le, T. Ahamad, T. T. Le, V.-H. Nguyen and P. Raizada, Flat meets functional: face-to-face 2D/2D S-scheme photocatalysts for efficient CO_2-to-fuel conversion, *Sustainable Energy Fuels*, 2025, **9**, 4832.

265 S. H. Osman, S. K. Kamarudin, M. H. Jamil, E. Alfianto, N. Shaari and Z. Zakaria, 3D Graphene-Coupled Aerogel Nanoarchitectures: Emerging Paradigm Toward Sustainable Applications in Fuel Cell, *Korean J. Chem. Eng.*, 2025, **42**, 2131.

266 H. Ali, *et al.*, Defect-driven innovations in photocatalysts: Pathways to enhanced photocatalytic applications, *InfoMat*, 2025, **7**, 70040.
267 S. H. Emon, M. I. Hossain, M. Khanam and D. K. Yi, Expanding Horizons: Taking Advantage of Graphene's Surface Area for Advanced Applications, *Appl. Sci.*, 2025, **15**(8), 4145.
268 J. Feng, S. Chen, Z. Lu and J. Bai, Metal–Organic Frameworks for Photocatalytic CO_2 Reduction: Progress and Prospects, *ACS Appl. Mater. Interfaces*, 2025, **17**, 60028.
269 J. Yu, G. Wang, B. Cheng and M. Zhou, Effects of hydrothermal temperature and time on the photocatalytic activity and microstructures of bimodal mesoporous TiO_2 powders, *Appl. Catal., B*, 2007, **69**, 171.
270 M. Tang, Y. Xia, D. Yang, J. Liu, X. Zhu and R. Tang, Effects of hydrothermal time on structure and photocatalytic property of titanium dioxide for degradation of rhodamine b and tetracycline hydrochloride, *Materials*, 2021, **14**, 5674.
271 T. T. P. N. X. Trinh, *et al.*, Hydrothermal synthesis of titanium dioxide/graphene aerogel for photodegradation of methylene blue in aqueous solution, *J. Sci.: Adv. Mater. Dev.*, 2022, **7**, 100433.
272 Aa Zhou, J. Bai, W. Hong and H. Bai, Electrochemically reduced graphene oxide: preparation, composites, and applications, *Carbon*, 2022, **191**, 301.
273 A. G. Marrani, A. Motta, F. Amato, R. Schrebler, R. Zanoni and E. A. Dalchiele, Effect of electrolytic medium on the electrochemical reduction of graphene oxide on Si(111) as probed by XPS, *Nanomaterials*, 2021, **12**, 43.
274 R. Y. N. Gengler, D. S. Badali, D. Zhang, K. Dimos, K. Spyrou, D. Gournis and R. J. D. Miller, Revealing the ultrafast process behind the photoreduction of graphene oxide, *Nat. Commun.*, 2013, **4**, 2560.
275 H. W. Cho and J. J. Wu, Photoreduction of graphene oxide enhanced by sacrificial agents, *J. Colloid Interface Sci.*, 2015, **438**, 291.
276 H. Singh, *et al.*, Revisiting the Green Synthesis of Nanoparticles: Uncovering Influences of Plant Extracts as Reducing Agents for Enhanced Synthesis Efficiency and Its Biomedical Applications, *Int. J. Nanomed.*, 2023, **18**, 4727.
277 Y. Wang, J. Yu, W. Xiao and Q. Li, Microwave-assisted hydrothermal synthesis of graphene based Au–TiO_2 photocatalysts for efficient visible-light hydrogen production, *J. Mater. Chem. A*, 2014, **2**, 3847.
278 P. Zhang, X. Teng, X. Feng, S. Ding and G. Zhang, Preparation of Bi_2WO_6 photocatalyst by high-energy ball milled Bi_2O_3–WO_3 mixture, *Ceram. Int.*, 2016, **42**, 16749.
279 L. Zhang, L. Jin, B. Liu and J. He, Templated growth of crystalline mesoporous materials: from soft/hard templates to colloidal templates, *Front. Chem.*, 2019, **7**, 22.
280 R. J. Li, W. J. Niu, W. W. Zhao, B. X. Yu, C. Y. Cai, L. Y. Xu and F. M. Wang, Achievements and Challenges in Surfactants-Assisted Synthesis of MOFs-Derived Transition Metal–Nitrogen–Carbon as a Highly Efficient Electrocatalyst for ORR, OER, and HER, *Small*, 2025, **21**, 2408227.
281 Z. Tong, Y. Hai, B. Wang, F. Lv, Z. Zhong and R. Xiong, Activated g-C_3N_4 Photocatalyst with Defect Engineering for Efficient Reduction of CO_2 in Water, *J. Phys. Chem. C*, 2023, **127**, 11067.
282 M. Mehrpooya and F. Bayatlar, Photocatalytic Reactors for CO_2 Reduction: Review on Simulation Studies, *Arch. Comput. Methods Eng.*, 2025.
283 Z. Sun, X. He and L. Duan, Multifunctional Soft and Solid Materials for Integrated CO_2 Capture and Utilization: Prospects and Opportunities, *Adv. Funct. Mater.*, 2025, e24549.
284 S. Chakraborty and S. C. Peter, Solar-Fuel Production by Photodriven CO_2 Reduction: Facts, Challenges, and Recommendations, *ACS Energy Lett.*, 2025, **10**, 2359.
285 M. Zhan, M. Xu, W. Lin, H. He and C. He, Graphene Oxide Research: Current Developments and Future Directions, *Nanomaterials*, 2025, **15**, 507.
286 M. Ramezani and O. Rahmani, A review of recent progress in the graphene syntheses and its applications, *Mech. Adv. Mater. Struct.*, 2024, **32**, 5256.
287 C. Amutha, A. Gopan, I. Pushbalatatha, M. Ragavi and J. A. Reneese, *Nanotechnology in Societal Development*, Springer, 2024, p. 481.
288 H.-Y. Zhuo, X. Zhang, J.-X. Liang, Q. Yu, H. Xiao and J. Li, Theoretical understandings of graphene-based metal single-atom catalysts: stability and catalytic performance, *Chem. Rev.*, 2020, **120**, 12315.
289 H. Chen, Y. Zheng, J. Li, L. Li and X. Wang, AI for nanomaterials development in clean energy and carbon capture, utilization and storage (CCUS), *ACS Nano*, 2023, **17**, 9763.
290 R. Awasthy, S. Flint, R. Sankarnarayana and R. L. Jones, A framework to improve university–industry collaboration, *J. Ind. Univ. Collab.*, 2020, **2**, 49.
291 N. Kalaiselvan and T. Mathimani, Solar-driven green hydrogen generation for revolutionizing the future of zero-carbon energy, *Fuel*, 2024, **375**, 132538.